

## GUIDELINES FOR PRACTICAL USE WHEN SHOTCRETING CLOSE TO BLASTING AND VIBRATIONS IN HARD ROCK

Anders Ansell

STIFTELSEN BERGTEKNISK FORSKNING  
ROCK ENGINEERING RESEARCH FOUNDATION

# **GUIDELINES FOR PRACTICAL USE WHEN SHOTCRETING CLOSE TO BLASTING AND VIBRATIONS IN HARD ROCK**

**Praktiska riktlinjer vid användning av sprut-  
betong nära sprängning och vibrationer i hårt  
berg**

Anders Ansell, KTH

BeFo Report 189  
Stockholm 2019  
ISSN 1104 – 1773  
ISRN BEFO-R—189—SE



# Preface

Rock construction in hard rock by blasting next to young sprayed concrete is common and needs to be developed with knowledge how the spray concrete is affected by vibrations. The uncertainty about the vibration levels that can be tolerated near freshly sprayed concrete often leads to overly conservative limit values being used in construction, with additional costs and planning uncertainties as a result.

The present report documents a project aimed at proposing practical guidelines for using shotcrete (sprayed concrete) near vibrations. The focus is on young and hardening wet-sprayed shotcrete for tunnels and civil engineering structures in hard rock and in the vicinity of blasting during the construction phase. The guidelines have been developed through numerical calculations and verified against observations, measurements and in situ results.

At KTH Concrete Structures, the project has been carried out by Anders Ansell (Professor). Appreciated support has been given by a reference group. The reference group consisted of Tommy Ellison (Besab), Rikard Gothäll (Tyréns), Martin Hansson (Sika Sweden), Henrik Ittnér (SKB), Daniel Johansson (LTU), Lars Malmgren (LKAB), Hans-Åke Mattson (ÅF), Mattias Roslin (Swedish Transport Administration) and Per Tengborg (BeFo). The project was financed by the Rock Engineering Research Foundation (BeFo).

Stockholm, 2019

*Per Tengborg*



# Förord

Bergbyggnad i hårt berg genom sprängning intill ung sprutbetong är vanligt förekommande och behöver utvecklas med kunskap hur sprutbetongen påverkas av vibrationer. Den osäkerhet som finns om de vibrationsnivåer som kan tolereras nära nysprutad betong leder ofta till att alltför konservativa gränsvärden används vid byggande, med merkostnader och planeringsosäkerheter som följd.

Föreliggande rapport redovisar ett projekt med syfte att föreslå praktiska riktlinjer vid användning av sprutbetong nära vibrationer. Fokus är på ung och hårdnande våtsprutad betong för tunnlar och anläggningar i hårt berg och i närheten av sprängningar under byggskedet. Riktlinjerna har framtagits genom numeriska beräkningar som verifierats mot observationer, mätningar och fältresultat.

Vid KTH Betongbyggnad har projektet genomförts av Anders Ansell (Professor i Betongbyggnad). Som stöd har funnits en referensgrupp som utfört ett uppskattat arbete. Referensgruppen bestod av Tommy Ellison (Besab), Rikard Gothäll (Tyréns), Martin Hansson (Sika Sverige), Henrik Ittnér (SKB), Daniel Johansson (LTU), Lars Malmgren (LKAB), Hans-Åke Mattson (ÅF), Mattias Roslin (Trafikverket) och Per Tengborg (BeFo). Projektet har finansierats av Stiftelsen Bergteknisk Forskning (BeFo).

Stockholm, 2019

*Per Tengborg*



# Summary

Uncertainty about the vibration levels that can be tolerated near newly sprayed concrete (shotcrete) often leads to excessively conservative limit values being used in the construction of tunnels and structures in rock, with additional costs and planning uncertainties as a result. Previously, it has only been possible to give general recommendations for safe vibration levels. A project with the aim of producing a set of practical vibration limit levels for shotcrete work close to blasting in hard rock has therefore been carried out. These recommendations span situations that may arise during "normal" construction in hard rock, and contain guidelines for safe distances and waiting times for newly sprayed shotcrete exposed to vibrations. In the project, the focus is on wet-mixed shotcrete on hard rock, of the type found in Sweden and Scandinavia.

A large number of calculations have been carried out with a previously developed and relatively computationally effective numerical elastic stress wave propagation model. As input data, various combinations of the weight of explosives, distance, rock type, shotcrete type, shotcrete age and thickness are used. For each combination of input parameters, the stresses that arise at the bond interface between rock and shotcrete have been calculated. The results are saved in a database and can be illustrated graphically with a 3D surface, as a function of shotcrete age and distance to the explosive charge. This surface has then been compared with another, which represents the growth of bond strength between rock and shotcrete. The intersection curve between the two surfaces represents the limit for safe blasting, taking into account combinations of shortest distances and the youngest allowable shotcrete at time of blasting.

The report contains a larger number of graphs showing limit values for safe blasting, which will be of value as reference in design work, enable comparisons with data from the field, and thereby feedback of experience. Based on the recommended limit values, dimensioning in the design stage will be made so that the results will be undamaged and safer shotcrete with longer life. Reduced need for re-spraying and repair leads to a high economic sustainability for large infrastructure projects and environmental sustainability when material consumption is reduced. The safety of tunnels and underground constructions will also be increased.

**Keywords:** Shotcrete, Tunnelling, Blasting, Vibrations, Distance, Age, Guidelines.





# Sammanfattning

Osäkerhet kring de vibrationsnivåer som kan tolereras nära nysprutad betong leder ofta till att alltför konservativa gränsvärden används vid byggande av tunnlar och berggrum, med merkostnader och planeringsosäkerheter som följd. Tidigare har det endast gått att ge generella rekommendationer för säkra vibrationsnivåer. Ett projekt med syfte att ta fram en uppsättning praktiska vibrationsgränsvärden för sprutbetongarbeten nära sprängning i hårt berg har därför genomförts. Dessa rekommendationer spänner över situationer som kan uppstå vid "normalt" byggande i hårt berg, och innehåller riktlinjer för säkra avstånd och väntetider för nysprutad vibrationsutsatt sprutbetong. Inom projektet studeras våtsprutad betong på hårt berg, av den typ som finns i Sverige och Skandinavien.

Ett stort antal beräkningar har genomförts med en tidigare framtagen och relativt beräkningseffektiv numerisk elastisk vågutbredningsmodell. Som indata används olika kombinationer av mängd sprängämne, avstånd, bergtyp, sprutbetongtyp, sprutbetongålder och tjocklek. För varje kombination av indataparametrar har sedan de spänningar som uppstår i vidhäftningsskiktet mellan berg och sprutbetong beräknats. Resultaten sparas i en databas och kan åskådliggöras grafiskt med en 3D yta, som funktion av sprutbetongålder och avstånd till laddningen. Denna yta har sedan jämförts med ytterligare en som representerar tillväxten av vidhäftningshållfastheten mellan berg och sprutbetong. Skärningslinjen mellan de två ytorna representerar gränsen för säker sprängning, beaktande kombinationer av kortaste avstånd och yngsta tillåtna sprutbetong vid tiden för sprängning.

Rapporten innehåller ett större antal diagram visande gränsvärden för säker sprängning, vilket kommer att vara av värde som referens vid projekteringsarbeten och också möjliggöra jämförelser med verifierande data från fältet och därigenom erfarenhetsåterföring. Utifrån de framtagna rekommenderade gränsvärdena kommer dimensionering i projekteringsstadiet att kunna göras så att oskadad och säkrare sprutbetong med längre livslängd fås. Minskat behov av omsprutning och reparation ger hög ekonomisk hållbarhet för stora infrastrukturprojekt och även miljömässig hållbarhet då materialåtgången minskas. Säkerheten i tunnlar och berggrum kommer också att höjas.

**Nyckelord:** Sprutbetong, Tunnelbyggnad, Sprängning, Vibrationer, Avstånd, Ålder, Riktlinjer.



# Contents

<b>1. Background</b> .....	<b>1.</b>
<b>2. Numerical model</b> .....	<b>3.</b>
2.1 Spring-mass mechanical model .....	3.
2.2 Previous results and recommendations .....	4.
2.3 Analysis strategy for guideline database .....	6.
<b>3. Rock properties</b> .....	<b>9</b>
3.1 Density and strength .....	9.
3.2 Elastic modulus and wave propagation .....	9.
3.3 Imperfections and cracks .....	11.
<b>4. Stress waves in rock</b> .....	<b>13.</b>
4.1 Vibration scaling laws .....	13.
4.2 Examples .....	14.
<b>5. Shotcrete properties</b> .....	<b>19.</b>
5.1 Measured modulus of elasticity .....	19.
5.2 Estimated modulus of elasticity .....	19.
5.3 Examples .....	20.
<b>6. Shotcrete-rock bond</b> .....	<b>23.</b>
6.1 Shotcrete on rock or concrete .....	23.
6.2 Mortar and concrete on rock or concrete .....	23.
6.3 Examples .....	24.

<b>7. Comparisons - previous and in situ results</b> .....	<b>27.</b>
7.1 The Kiruna tests .....	27.
7.2 The Södra länken tests .....	32.
7.3 Previous numerical results .....	34.
7.4 Large scale blasting .....	36.
<b>8. Conclusions and recommendations</b> .....	<b>39.</b>
<b>Bibliography</b> .....	<b>41.</b>
<b>Appendix A Input data</b> .....	<b>45.</b>
<b>Appendix B Recommended vibration limits</b> .....	<b>49.</b>

# Chapter 1

## Background

During tunnelling and construction in hard rock using the drill and blast method, each detonation of explosives gives rise to stress waves that propagate through the rock. As these reach a free rock surface or tunnel wall, damage to shotcrete sprayed on the rock surface may occur. This can be a big problem if blasting occurs early after shotcreting and at short distances. The amplitude of the waves is directly proportional to the vibration velocity of the material particles that are set in motion by the energy released from the detonation. The term peak particle velocity ( $ppv$ ) is often used to indicate the maximum vibration level. However, this velocity should not be mistaken for the propagation velocity of stress waves, which depends on the properties of the rock material and indicates how fast the wave front moves through the rock material. Cracks in the rock act as mechanical filters, where some of the wave energy are reflected away with the frequency content affected, see e.g. Dowding (1996). It has not been fully confirmed but the occurrence of cracks in rock immediately under shotcrete should therefore have an advantageous effect on its vibration resistance to incoming stress waves.

Shotcreting is often done immediately after drilling and blasting, to quickly secure the shape of the rock surface by preventing smaller blocks and stones from falling out. This ensures that e.g. the arch shape of a tunnel is maintained so that the rock can carry its own weight as intended. Because of this, the shotcrete's ability to bond to a rock surface and the so-called mortar effect are of great importance. The latter means that the shotcrete upon impact penetrates cracks and small cavities in the rock. Today it is common to use set-accelerators when fast hardening and rapid strength growth is desirable for shotcrete. This is especially the case when using wet-mixed shotcrete at a larger scale, which is the focus of this report. Short waiting times between blasting rounds are important for an efficient construction process. Therefore, knowledge of safe blasting limits - in time and distance - is important for safe constructions. Knowledge on how shotcrete should be designed to withstand damage from vibrations is fundamental for a long service life, good durability and thus a low environmental impact. An increase in knowledge will result in significantly fewer cases of vibration-damaged shotcrete supports, thereby reducing the need to replace heavily damaged shotcrete sections already during the construction phase. A reduced need for re-spraying and repairs are highly relevant for the economic and environmental sustainability of large infrastructure projects.

Today, there are only general guidelines for practical use and these are often based on the development of compressive strength or as maximum allowed  $ppv$ -levels. Limit values for vibration near cast mass concrete are not directly applicable, as the wave reflections in the thin, bonding shotcrete shells are not comparable to those in 3D concrete volumes, see e.g. Ansell & Silfwerbrand (2003). For shotcrete, some indicative guidelines have been published, see for example Ansell (2005, 2007ab). However, the number of combinations of parameters such as shotcrete age and thickness, rock properties, amount of explosives and distance are relatively few and not enough to establish a set of detailed guidelines for practical use.

This project have therefore been initiated, for compiling a database of practical vibration levels for shotcrete work close to blasting in hard rock, of the type primarily found in northern Europe, i.e. Sweden and Scandinavia. These recommendations focus on situations that may arise during construction in hard rock and will provide safe distances and waiting times for newly sprayed wet-mix shotcrete subjected to blasting vibrations. A large number of calculations are carried out with a previously developed and relatively computationally effective numerical elastic wave propagation model. The database systematically compiled from the results will show relationships between the amount of explosives, distance, rock type, shotcrete type, age and thickness. It will be of great value as reference for design work and facilitate comparisons with in situ data and thus also generate experience feedback.

# Chapter 2

## Numerical model

The vibration resistance of newly sprayed and hardening shotcrete have previously been investigated through in situ measurements and observations and by using analytical and numerical modelling. Relatively few in situ investigations have focused on finding the damage limit since this must involve the destruction of shotcreted tunnel walls, which is costly. There are some studies where vibration measurements that has been performed during tunnel blasting that resulted in intact shotcrete, i.e. a confirmation on that the low amount of explosives used did not damage nearby newly sprayed shotcrete. However, to identify damage levels, numerical and analytical investigations must be performed and the results verified through comparison with in situ results. In the following sections, the previous work is briefly summarized and the analytical strategy adopted for the present project outlined.

### *2.1 Spring-mass mechanical model*

To gain understanding of the failure mechanisms involved and to be able to study the influence from variations in important parameters, a series of analytical and numerical modelling studies have been carried out. The tests were first numerically evaluated based on elastic stress wave theory, with a model for one-dimensional analysis of shotcrete on rock through which elastic stress waves propagate (James, 1998 and Ansell, 1999). This was followed by investigations using mechanical spring-mass models for the dynamic analysis (Ansell, 2005, 2007ab and Nilsson, 2009). These models were one-dimensional, with concentrated masses and springs, and two-dimensional, with elastic beams and distributed spring-beds. The latter model is two-dimensional which facilitates the calculation of a two-dimensional displacement field instead of the displacement at an isolated node, thus considering the effects of longitudinal (P-) waves and shear (S-) waves in combination. The beam elements represent the flexural stiffness and mass of the shotcrete and the fractured rock closest to the rock surface, with spring elements added to obtain elastic coupling between shotcrete and rock. It has been shown (Ahmed & Ansell, 2012a) that all these three model types give comparable results, but with differences in computational time, amount of input data needed and the detail level of the output data produced.

For the present project, where a large number of calculations must be carried out effectively and systematically, the one-dimensional mass-spring model have been chosen, see Figure 2.1. The model have degrees of freedom (dof) in the direction of the P-wave propagation, describing the vibration of a unit area of the shotcrete layer using lumped masses connected through elastic springs. Typically, twenty dofs ( $u_1-u_{20}$ ) are assigned for the model. It should be noted that for clarity, only 2 dofs are included in Figure 2.1. The analysis is performed in the same manner as an earthquake analysis, see e.g. Clough & Penzien (1993). Here, the rock corresponds to the vibrating ground and the shotcrete layer is the structure for which the response is to be determined. The model represents a unit area of shotcrete and describes



its displacement and deformation due to the vibrating rock surface ( $u_g$ ). The mass of the shotcrete is lumped, i.e. divided into point-masses ( $m_{\text{shcr}}$ ) concentrated to the nodes where the dofs are located. The elongation and shortening of the elastic springs corresponds to the stress states within the shotcrete layer. The stiffness of the springs ( $k_{\text{shcr}}$ ) is calculated with respect to the elastic modulus of the shotcrete that here will vary as the shotcrete hardens with age. The bond stress at the shotcrete-rock interface correspond to the elongation of the (upper) spring that anchors the shotcrete in the rock surface. The time-dependent displacement  $u_g$  of the rock surface is assigned as a ground acceleration, calculated on basis of the estimated maximum vibration velocity for one particle, the so-called peak particle velocity ( $ppv$ ). This measure is often used as vibration criterion and is here further discussed in section 4.1. If the direction of vibration in the model is  $x$  in an orthogonal 2D  $xy$ -system, the ground acceleration caused by the blasting can be assumed to be a sine wave, following:

$$u_{gx}(t) = 2\pi f \cdot v_{max} \cdot \cos\left(\arctan\frac{R_x}{R}\right) \cdot \sin(2\pi ft) \quad (2.1)$$

where it should be understood that vibrations in the  $y$ -direction, parallel with the shotcreted surface, here is omitted. In the equation,  $t$  is time,  $f$  the vibration frequency that depend on the characteristics of the rock, the  $ppv$  which is  $v_{max}$ , the direct distance  $R$  between shotcrete and explosive charge and its component  $R_x$  in the  $x$ -direction, respectively.

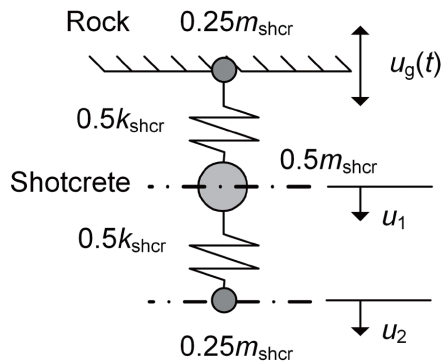


**Figure 2.1:** One-dimensional mass-spring mechanical analysis model. From Ahmed & Ansell (2012a).

## 2.2 Previous results and recommendations

Examples of previously calculated numerical results are shown in Figures 2.2–2.3. Both figures presents calculated results from detonation of 2 kg of explosives in hard rock and close to shotcrete with a thickness of 25, 50 or 100 mm. The curves that represent bond  $\sigma_{bd}$  stresses at the shotcrete-rock interface are compared with curves representing bond strength  $f_{bd}$  and in Figure 2.3 also with tensile strength  $f_{ct}$ . However, the latter will for most practical cases be higher than the bond strength and the critical failure mode will be loss of bond between rock and shotcrete. The curves from the two figures, that represent one case with varying distance and one with varying shotcrete age, are used for comparison in section 7.3. This far, some recommendations for practical use have been given based on a relatively limited number of studied cases of this type, see e.g. Ansell (2005) and Ansell (2007a).

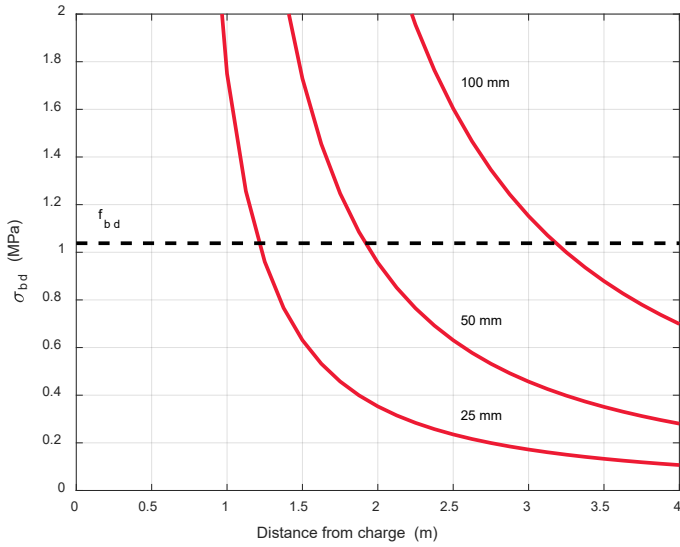


**Figure 2.2:** Calculated shotcrete bond stress from  $Q=2$  kg explosives for 28 days old shotcrete (Ansell, 2005).

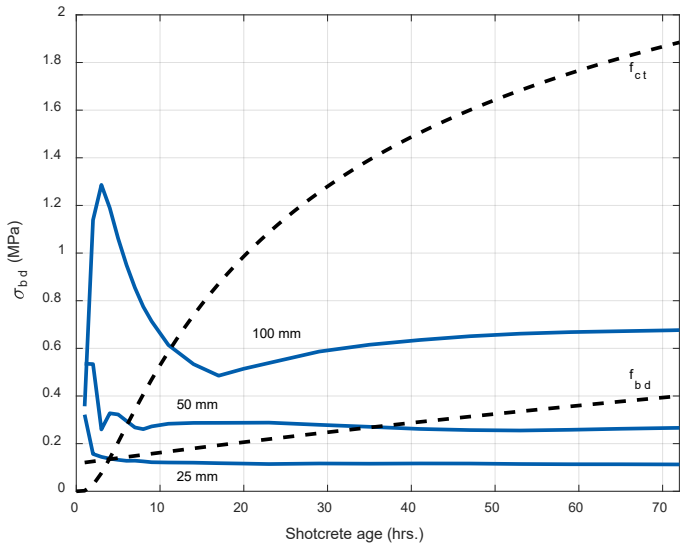


**Figure 2.3:** Calculated shotcrete bond stress from  $Q=2$  kg explosives for hardening shotcrete at 4 m distance (Ansell, 2007a).

### ***2.3 Analysis strategy for guideline database***

Through systematic combination of variations in explosive charge weight, shotcrete thickness and rock type, and by performing numerical calculations covering many practical cases found in situ, a database will be set up that contains limit values that can be used for practical design and planning for hard rock blasting close to young and newly sprayed shotcrete. The numerical work involved consist of a large number of calculations for combinations of the governing parameters, varying within ranges that usually occur in tunnelling and rock construction work.

The approach is demonstrated in Figure 2.4. For a constant combination of explosive charge weight, shotcrete thickness and rock type (modulus of elasticity and density), calculations of tensile stresses in the shotcrete-rock bond interface are performed for combinations of distance and shotcrete age, i.e. increasing modulus of elasticity. For each combination of input parameters, a calculation with the numerical model presented in section 2.1 is performed. To, for example, generate the results shown in Figure 2.4, approximately 1000 calculations are required that each identifies the maximum stress that occurs in the bond interface for one particular combination of input parameters.

Thus, in the first calculation step, a 3D surface is created which describes the relationships between shotcrete age - distance - bond stresses. In a second calculation step, for the same combinations of shotcrete age - distance, a 3D surface is created which describes the growth in rock-shotcrete bond strength. The third calculation step consists of plotting these two surfaces in the same 3D coordinate system, where the intersection between these is of particular interest. This 3D curve indicate the safe vibration levels so that the points beyond the curve are safe combinations of distance - shotcrete ages when blasting with the prescribed amount of explosives are done for the assumed rock and shotcrete types. In a fourth calculation step, the limit curve can be isolated and stored numerically as three vectors, or alternatively a 3D curve fitting can be made after which the curve parameters are saved. The results can also be relatively easily illustrated in 2D diagrams showing distance - shotcrete age, distance - bond stress or shotcrete age - bond stress.

Through the procedure described, by systematically combining input parameters, a database that covers large variations of design parameters can be built up relatively effectively. Through numerical post-processing routines, limit values for any combination of input parameters within the ranges considered can then be extracted. The sections 7.1–7.4 provide examples of how the method can be applied and in sections 3.1–6.2 there are discussions on how the required input parameters should be chosen.

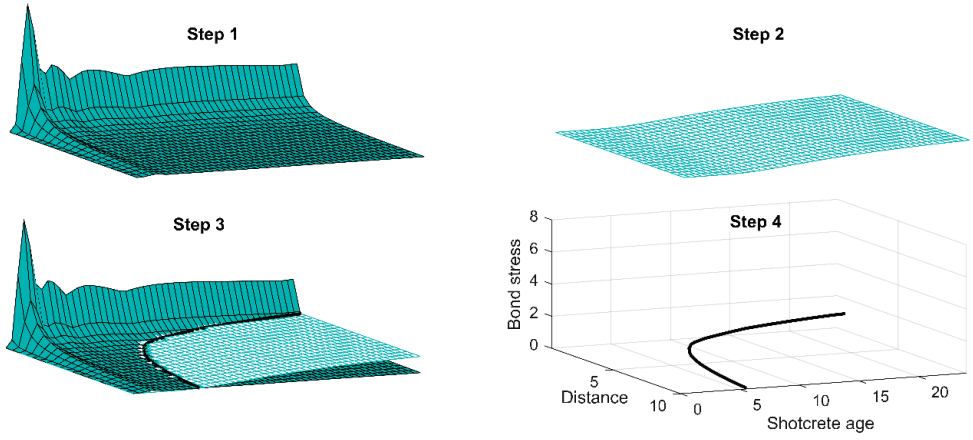


**Figure 2.4:** *Computation procedure; (1) bond stresses, (2) bond strength; (3) intersection between surfaces and (4) limiting curve.*



# Chapter 3

## Rock properties

The following sections summarize relevant material properties for hard rock types common in Sweden and Scandinavia. The selection is also made on basis of the previous research within the field of shotcrete exposed to vibrations in hard rock. If no other references are given for the source, the following tabulated values are based on the Swedish handbooks Bygg 1A (1971), Bygg 1B (1971) and Bygg T (1990), and the course books within the field of rock mechanics, by Stille & Nord (1990) and Bodare (1997).

### 3.1 Density and strength

Density and compressive strength for a selection of rock types are given in Table 3.1. These are representative for average qualities of Granite and Gneiss, but also Sandstone is included for comparison. As important in situ tests with young shotcrete has been carried out in the Kiruna mine in northern Sweden (see section 7.1), values for the Magnetite and Syenite in the mine are added to the compilation.

**Table 3.1:** *Properties of a selection of rock types – densities and compressive strengths.*

Rock type	Density (kg/m <sup>3</sup> )	Compressive strength (MPa)	References
Gneiss	2700	160-280	
Granite	2500-2800	160-240	
Södra Länken	2500	Unknown	Reidarman & Nyberg (2000)
Sandstone	2100-2700	30-118	
Kiruna, Magnetite	4800	120	Nyberg & Fjellborg (2000) Jinnerot & Nilsson (1998)
Kiruna, Syenite	2715	300	Nyberg & Fjellborg (2000)

### 3.2 Elastic modulus and wave propagation

For dynamically loaded rock, for example with stress waves from blasting, the wave propagation velocity and elastic modulus are other important material properties. For the numerical model shown in section 2.1, the elastic modulus of rock are used to calculate the wave propagation velocity which is relevant for determining the characteristic frequency of the load, which is further discussed in the following section.

For the same rock types as in Table 3.1, these dynamically relevant properties are summarized in Table 3.2. The wave propagation velocities listed are that of longitudinal (P-) waves, since the direction of particle vibration in these coincide with the dofs assigned to the numerical model in Figure 2.1.

For waves in an elastic medium with the density  $\rho$ , see e.g. Dowding (1996), the P-wave velocity is calculated as:

$$c_p = \sqrt{\frac{E}{\rho}} \quad (3.1)$$

while the velocity of shear (S-) waves is given by:

$$c_s = \sqrt{\frac{G}{\rho}} \quad (3.2)$$

The relation between the elastic modulus  $E$  and modulus of shear  $G$  depend on Poisson's ratio  $\nu$ , according to:

$$G = \frac{E}{2(1+\nu)} \quad (3.3)$$

For example, the Magnetite in the Kiruna mine have a ratio that is  $\nu = 0,25$  (Malmgren, 2001), which gives  $E = 2,5G$  and a shear wave propagation velocity of  $c_s \approx 4000$  m/s, to be compared to the higher value for  $c_p$  that is given in Table 3.2.

The modulus of elasticity for intact granite is in the range 40–80 GPa (Ansell, 2007a), but due to the heterogeneous nature of the rock a lower average value is often assigned to a larger rock mass. In the study by Ahmed et al. (2012) the modulus was set to be within 16–40 GPa. The higher limit thus corresponds to high quality intact rock while the lower corresponds to a slightly fractured rock mass (Bieniawski, 1978). The elastic modulus for intact Magnetite rock in the Kiruna mine is in the range 40–110 GPa (Ansell 2007 b), which can be compared to that of low quality granite, see Ansell (2005, 2007a). In Table 3.2, some values for the elastic modulus is approximative and put within brackets as these do not correspond to in situ measured values but instead to the theoretical relation given by Eq. (3.1), i.e. they correspond to upper limits for small and un-cracked samples. For larger rock volumes containing more imperfections it can be motivated to in some cases use an even lower modulus, see e.g. Ansell (2007b). The importance of rock cracks are further discussed in the following section.

**Table 3.2:** *Properties of a selection of rock types – elastic moduli and elastic stress wave propagation velocities.*

Rock type	Elastic modulus (GPa)	Wave propagation velocity (m/s)	References
Gneiss	30-100	3500-7000	
Granite	40-80	3500-7000	
Södra Länken	(appr. 70)	5300	Reidarman & Nyberg (2000)
Sandstone	3-60	2500-3500	
Kiruna, Magnetite	(appr. 190)	6270	Nyberg & Fjellborg (2000)
		6318	Jinnerot & Nilsson (1998)
Kiruna, Syenite	(appr. 90)	5800	Nyberg & Fjellborg (2000)

### 3.3 Imperfections and cracks

In rock, layers and cracks will have a filtering effect on vibration waves propagating in the rock due to waveguide effects. This means that certain frequencies within a frequency spectrum of a vibration signal will be amplified while others will be damped out, depending on the characteristics of the medium, often fractured rock or layered soil. The distance between cracks  $H$  is used to calculate a characteristic frequency for the numerical model presented in section 2.1. An equation where the amplified frequency  $f$  depends on the layer thickness  $H$  and wave propagation velocity  $c$  is given by Dowding (1996), as:

$$f = \frac{c}{4H} \quad (3.4)$$

A similar expression is given by Bodare (1997), as:

$$f_n = \frac{c}{4H}(2n+1) \quad n = 0, 1, 2, \dots \quad (3.5)$$

where the frequencies  $f_n$  are called resonance frequencies, that are amplified while passing the medium. The characteristic frequency is here used as input for the numerical modelling the calculation of the rock surface acceleration given by Eq. (2.1).

For fractured or cracked rock, local variations in the distance between cracks are to be expected. For the Kiruna mine, Malmgren (2001) gives the interval  $H \approx 0,2-0,6$  m for the distance between cracks in the rock mass. For the study by Ahmed & Ansell (2014) a section of 0,5 m thick slightly fractured rock was assumed along the tunnel walls. In the numerical model used, this was also represented by a low modulus of elasticity, chosen as 16 GPa that is in accordance with the observations by Bieniawski (1978).

An example of damage criterion for Swedish hard rock is given by Persson (1997), where the threshold damage (incipient damage) occurs at a peak particle velocity ( $ppv$ ) of 1000 mm/s. The damage depth in rock from different amount of explosives can be calculated using empirical formulas for the relation between  $ppv$ , distance and explosive charge weight, see section 4.1. As an example for granite, the empirical relation from Table 4.1, case 1 will give the limit distance for rock damage based on this threshold value that becomes:

$$R_{ppv} = 0,788\sqrt{Q} \quad (\text{m}) \quad (3.6)$$

Over this limit distance from the explosive charge, the rock can be assumed to be without major cracks caused by the blasting.





# Chapter 4

## Stress waves in rock

The magnitude of the stress waves, i.e. the particle vibration velocities, that arise in rock following an explosion depends on the weight of the explosives, the distance to the point of observation and the properties of the rock. The particle velocities that can be measured remote from a detonation in rock will show a decrease in magnitude with increasing distance to the source of explosion. This decay is caused by geometrical spreading and hysteretic damping in the rock (Dowding, 1996).

### 4.1 Vibration scaling laws

Basic expressions for the *ppv*, i.e. the maximum particle vibration velocity  $v_{\max}$  (in mm/s), is given as a scaling law put forth by Holmberg & Persson (1980), and others, on the form:

$$v_{\max} = v_1 \cdot \frac{Q^a}{R^b} \quad (4.1)$$

where the distance to an explosive charge  $R$  is in m and the weight of the explosives  $Q$  in kg. The constants  $a$  and  $b$  depend on geometry and rock properties. The factor  $v_1$  is often called the “intercept” and is the particle velocity for  $Q^a/R^b = 1$ . In this scaling law, the relation between the constants  $a$  and  $b$  is often chosen as either  $b = 3a$ , giving a cube-root scaling relationship, or  $b = 2a$ , a square-root relationship. Here, the latter will be chosen due to that long explosive charges are expected to be in use for hard rock tunnelling, giving rise to wave fronts that propagate as expanding cylinders, i.e. in two dimensions. For a thorough discussion of the features of the two approaches, see e.g. Dowding (1996). The choice of square root scaling leads to:

$$v_{\max} = v_1 \cdot \left( \frac{R}{\sqrt{Q}} \right)^{-b} \quad (4.2)$$

which can be represented by a straight line in a log–log scaled plot with  $v_{\max}$  as function of the scaled distance  $R/\sqrt{Q}$ .

When using the scaling equations for calculations of vibration velocities from long explosive charges at short distances, the equation needs to be modified to give accurate predictions for long charges by reducing  $Q$  (Ouchterlony et al., 1993):

$$v_{\max} = v_1 \cdot \left( \frac{R}{\sqrt{f \cdot Q}} \right)^{-b} \quad (4.3)$$

The reduction factor  $f$  includes the length of the explosive charge  $L_c$  and  $R$  which is the distance between the charge centre and the point of observation:

$$f = \frac{\arctan(L_c / 2R)}{(L_c / 2R)} \quad (4.4)$$

## 4.2 Examples

In the following are some examples of scaling relationships from the literature compiled and commented. These have been chosen to represent typical hard rocks of the kind found in Sweden and Scandinavia, and because they relate to previous, relevant research and in situ measurements. The examples are summarized in Table 4.1, where the original reference is given as source of information and with references to research papers where the relation has been used also listed. Common for the relationships listed is that they are based on square root scaling, as discussed above. The expressions are in the form given by Eq. (4.2) above.

Scaling laws for typical Swedish bedrock of granite type is given by e.g. Ouchterlony et al. (1993), that sets the constants to  $b=1,50$  and  $v_1 = 700\text{--}1000$  mm/s. One example for gneiss is given by Lundborg et al. (1978), from vibration measurements done in a quarry at Brännland close to Umeå in northern Sweden, resulting in  $b = 1,60$  and  $v_1 = 780$  mm/s. In the Södra Länken road tunnels in Stockholm, Reidarman & Nyberg (2000) established that in  $b=1,40$  and  $v_1 = 700$  mm/s. From the measurements in the Kiruna mine (Ansell, 1999), the values representative for the iron-ore (magnetite) was found to be  $b= 1,38$  and  $v_1 = 832$  mm/s. An investigation at a different site within the mine (Jinnerot & Nilsson, 1998), resulted in results closer to that of granite with  $b = 1,70$  and  $v_1 = 700$  mm/s. However, these measurements may have been carried out outside the actual ore-body within the mine. Measurements in the mine by Nyberg & Fjellborg (2000) gave values for  $b$  and  $v_1$  that were 0,93–1,73 and 380–850 mm/s, respectively, in the magnetite. In the nearby waste rock (Syenite) the corresponding values were 1,34–1,40 and 860–720 mm/s, respectively

The twelve scaling relationships given in Table 4.1 are illustrated in Figures 4.1–4.3, plotted in different scales. It should be noted that the log-log plot in Figure 4.3 represent the most common type of plot, with the distance  $R$  scaled with the explosive charge weight  $Q$ .

**Table 4.1:** *Compilation of vibration scaling laws. Coefficients for  $v_{\max} = v_1 \cdot (R / \sqrt{Q})^{-b}$  (mm/s).*

	Source	$v_1$ (mm/s)	$b$	$\rho$ (kg/m <sup>3</sup> )	$c_p$ (m/s)	Rock type	Comments Used in in ref.
1	Ouchterlony et al. (1993)	700	1,50	2500-2800	3500-7000	Swedish bedrock (min)	Ansell (2005, 2007a) Ahmed & Ansell (2012a)
2	Reidarman & Nyberg (2000)	900	1,50	2500-2800	3500-7000	Swedish bedrock (max)	
3	Ouchterlony et al. (1993)	1000	1,50	2500-2800	3500-7000	Swedish bedrock (max)	
4	Lundborg et al. (1978)	780	1,60	2700	3500-7000	Brännland quarry - Gneiss	
5	Reidarman & Nyberg (2000)	700	1,40	2500	5300	Södra Länken	Assumed similar properties as Syenite. Ahmed & Ansell (2014)
6	Reidarman & Nyberg (2000)	700	1,40	2715	5800	Syenite - Kiruna	
7	Nyberg & Fjellborg (2000)	860	1,34	2715	5800	Waste rock (Syenite?) – Kiruna	
8	Nyberg & Fjellborg (2000)	720	1,40	2715	5800	Waste rock (Syenite?)– Kiruna	
9	Nyberg & Fjellborg (2000)	850	1,73	4800	6270	Iron ore (Magnetite) - Kiruna	
10	Nyberg & Fjellborg (2000)	380	0,93	4800	6270	Iron ore (Magnetite) - Kiruna	
11	Jinnerot (1998)	700	1,70	4800	6318	Iron ore (Magnetite) - Kiruna	Ansell (1999, 2007b)
12	Ansell (1999)	832	1,38	4800	6318	Iron ore (Magnetite) - Kiruna	Ansell (2004)

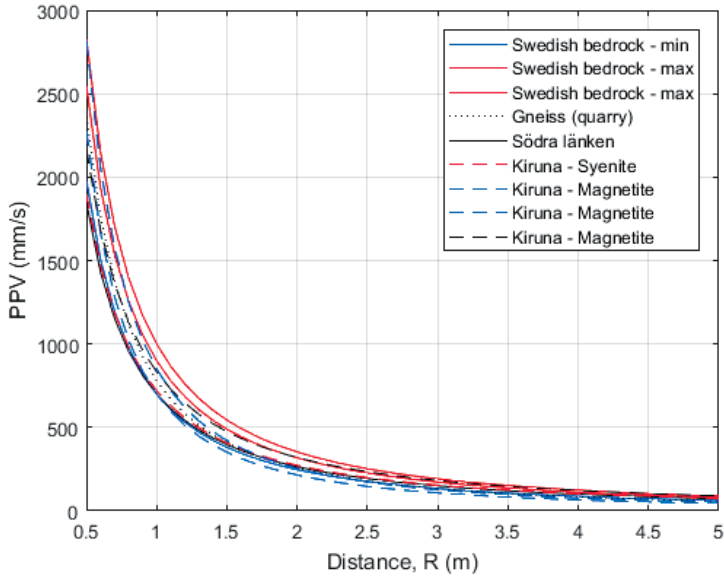


**Figure 4.1:** Scaling laws in hard rock – for  $Q = 1$  and  $3$  kg of explosives.

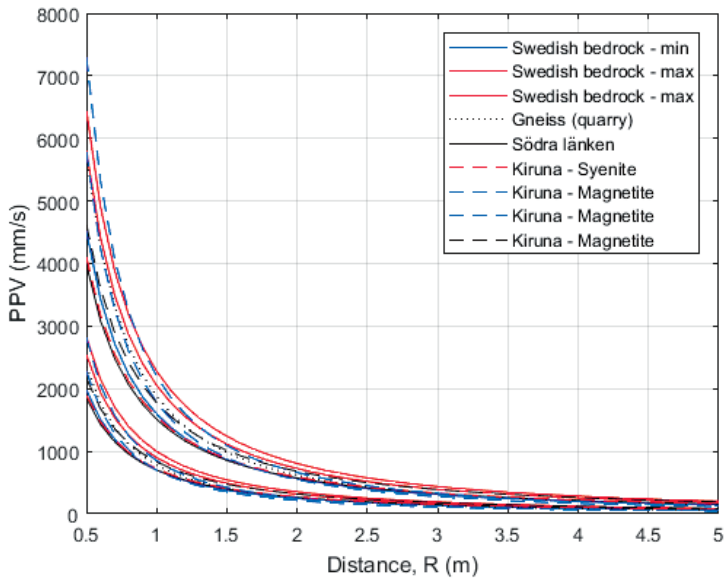


**Figure 4.2:** Scaling laws in hard rock – for  $Q = 1$  kg of explosives.

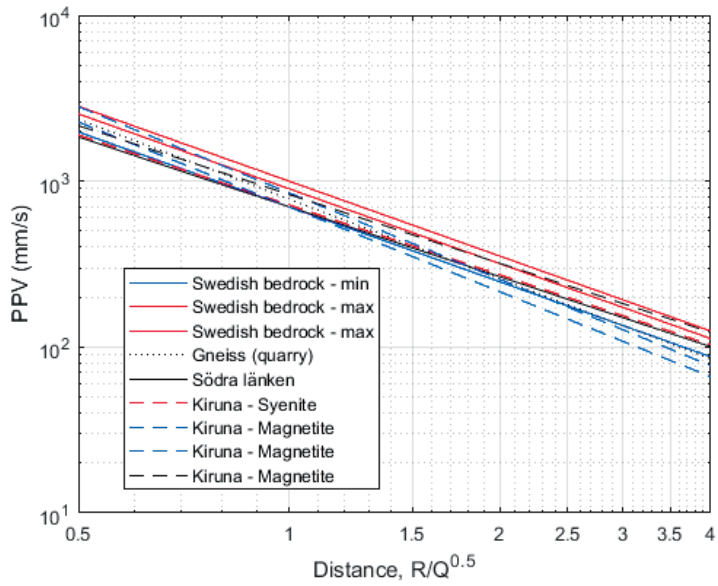


**Figure 4.3:** *Scaling laws in hard rock – scaled distances in log-log scale.*



# Chapter 5

## Shotcrete properties

Important shotcrete parameters used as input for the numerical model described in section 2.1 is density and thickness, which together gives the mass of the vibrating dynamic system. The stiffness properties are in the model represented by spring stiffness that is calculated on from the elastic modulus of the shotcrete. It should be noted that the elastic modulus of a dynamically loaded material can be effected by strain-rate effects and damping but these effects are here minor due to the the loading rates and the relatively short duration of loading. However, it must be noted that little or no research have been done on these effects on shotcrete. Young and hardening shotcrete is studied and therefore is the development of the elastic modulus with shotcrete age of interest. For evaluation of the calculated results may also the age dependent tensile strength be of interest. Thus, the age dependent property most often investigated, i.e. the compressive strength, is not directly used in the modelling but may be the basis for approximation or estimation of the tensile strength and elastic modulus in cases when information on these are missing.

### *5.1 Measured modulus of elasticity*

There are relatively few presented expressions for the development of the elastic modulus  $E$  for very young and hardening shotcrete that originates from direct in situ measurements. An average expression, calculated as a mean value based on a literature survey, is given by Chang (1994). The equation is valid for a “normal” shotcrete where  $E$  reach 27 GPa after 28 days. However, it must be remembered that this today may not be fully representative for an average, wet-sprayed shotcrete due to e.g. the introduction of modern set-accelerators, newer cement types and progress within the spraying technology. Based on laboratory measurements, Meschke (1996) gives an expression based on that given in CEP-FIP model code 1990 (1991), which is valid up to 28 days where after  $E$  is assumed to be constant,  $E = 28$  GPa. The expression given by Oreste and Pelia (1997) is valid for shotcrete with  $f_c = 35$  MPa at 28 days of age. Three expressions, derived from testing of shotcrete with different compositions, are given by Pöttler (1990). Based on laboratory testing by several researchers, Neuner et al. (2017) derive a theoretical expression for shotcrete with  $E = 21,5$  GPa at 28 days.

### *5.2 Estimated modulus of elasticity*

When in situ or laboratory data is scarce or missing the elastic modulus can be evaluated from the corresponding and by measurements known compressive strength. However, the empirical relations often used are for cast concrete and it is not investigated how this relation possibly varies with concrete,



or shotcrete, age. However, one average expression for the shotcrete modulus of elasticity as function of the compressive strength  $f_c$  is given by Chang (1994), and used e.g. by Ansell (2007a). The expression is also used to estimate the elastic modulus from the compressive strength measured in situ in the Kiruna mine (Ansell, 1999). The equation is calculated from a large number of investigations and is:

$$E = 3,86 f_c^{0,60} \text{ (GPa) with } f_c \text{ in MPa} \quad (5.1)$$

This equation is also used by Bryne et al. (2014), to estimate the elastic modulus from laboratory tests on young and hardening shotcrete. Apart from the bond strength (see section 6.1) also the development of the compressive strength with shotcrete age was investigated. The tests were performed at +20 °C but to facilitate comparison with the bond strength results curves adjusted to represent +7 °C are also presented. The latter are obtained by using the maturity function (the TT-method) in the form used by Byfors (1980), resulting in a stretched time axis (multiplication with 1,765) that corresponds to the lower temperature. The instant effect of the set accelerator was not captured but the compression strength should be around 2–3 MPa directly after shotcreting, according to Lagerblad et al. (2006).

### 5.3 Examples

The time dependent growth of the elastic modulus as presented and suggested in the references cited in the previous two sections are plotted for comparison in Figures 5.1–5.2. The expressions for the plotted curves are summarized and given in Eqs. (5.2–5.12). The shotcrete age  $t$  is here given in hours, which for some have involved a re-calculation from the version presented in the original reference. The elastic modulus  $E$  is in GPa and, unless specifically stated, the expressions are valid for ages up to at least 72 hours.

An average relation for hardening shotcrete where  $E$  after 28 days is 27 GPa is given by Chang (1994):

$$E = 1,062 \cdot 27 e^{-4,12/t^{0,70}} = 28,7 e^{-4,12/t^{0,70}} \quad (5.2)$$

A variation on this equation was used in the numerical study by Ahmed et al. (2012):

$$E = 1,062 \cdot 27 e^{-5,67/t^{0,80}} = 28,7 e^{-5,67/t^{0,80}} \quad (5.3)$$

A second average expression is presented by Chang (1994), derived from the relation to compressive strength given by Eq. (5.1):

$$E = 31,8 e^{-5,53/t^{0,60}} \quad (5.4)$$

Also derived from Eq. (5.1) and from in situ compressive strength measurements from Kiruna (Ansell, 1999) is:

$$E = 24,3 e^{-3,84/t^{0,60}} \quad (5.5)$$

An expression based on the CEP-FIP model code 1990 (1991), with  $E$  at 28 days that is 28 GPa and then constant, is put forth by Meschke (1996):

$$E = 28 \left( 0,85 + \frac{100,8}{t} \right)^{-0,5} \quad (5.6)$$

For shotcrete with  $f_c = 35$  MPa at 28 days, the following is suggested by Oreste and Pelia (1997):

$$E = 28(1 - e^{-0,0187t}) \quad (5.7)$$

Three expressions for shotcrete of different strengths are presented by Pöttler (1990), first for a weaker shotcrete with  $E = 20$  GPa at 28 days:

$$E = 1,062 \cdot 20e^{-3,00/t^{0,60}} = 21,2e^{-3,00/t^{0,60}} \quad (5.8)$$

Then for a stronger shotcrete with  $E = 30$  GPa at 28 days:

$$E = 1,084 \cdot 30e^{-4,01/t^{0,60}} = 32,5e^{-4,01/t^{0,60}} \quad (5.9)$$

and finally for a very strong shotcrete with  $E = 40$  GPa at 28 days:

$$E = 1,232 \cdot 40e^{-6,17/t^{0,60}} = 49,3e^{-6,17/t^{0,60}} \quad (5.10)$$

The following expression, presented by Neuner et al. (2017), is for shotcrete with  $E = 21,5$  GPa at 28 days:

$$E = 21,5e^{0,101(1-\sqrt{672/t})} \quad (5.11)$$

From the experimental tests by Bryne et al. (2014), the following expression has been estimated using Eq. (5.1), from compressive strengths measured at +20 °C:

$$E = 30,2e^{-397,0/t^{2,17}} \quad (5.12)$$

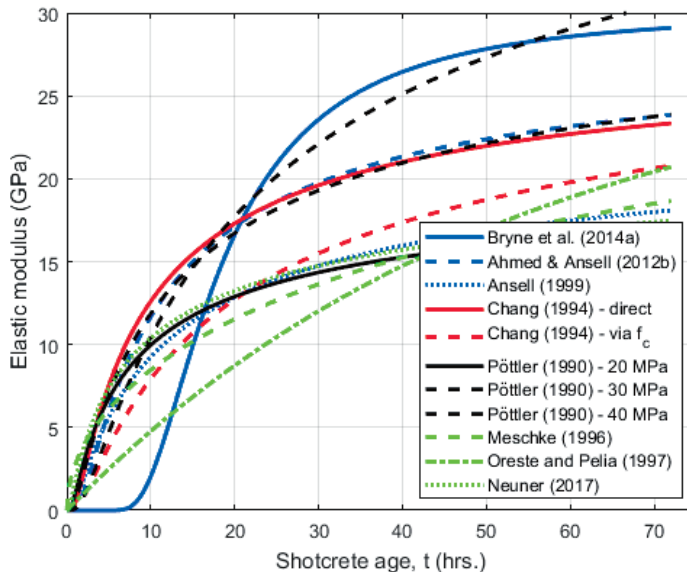


**Figure 5.1:** Elastic modulus of shotcrete.

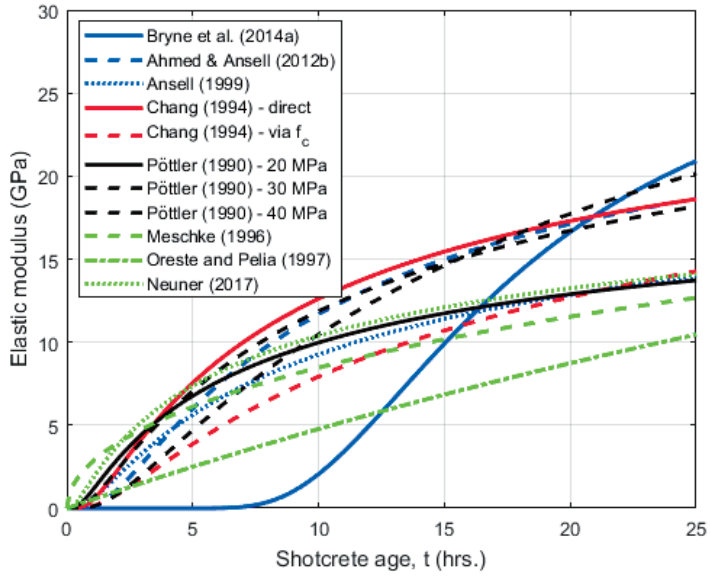


**Figure 5.2:** Elastic modulus of shotcrete.

# Chapter 6

## Shotcrete-rock bond

The bond strength between fully hardened shotcrete and rock is usually determined through pullout tests in the direction perpendicular to the rock wall. These in-situ tests usually give results between 0 and 2 MPa but at conditions normal for tunnelling, values higher than 0,5 MPa are realistic. There are almost no reliable test results published on the development of the bond strength for hardening shotcrete on rock. The strength have to be based on comparisons with results from few in situ observations and laboratory tests, as shown in the following sections.

### *6.1 Shotcrete on rock or concrete*

The bond strength between shotcrete older than 28 days and various types of rock is presented by Hahn (1983) and Hahn and Holmgren (1979). A compilation of guidelines is put forth by Malmberg (1992), who summarizes the often used limits for bond between shotcrete and rock as 1–2 MPa, which is of similar size as between concrete layers. A maximum value of 0,5 MPa for practical use as bond strength between shotcrete and hard granite is according to Malmberg (1992) given by Vandevallé (1996).

During in-situ tests at the Kiruna mine (Ansell, 1999), pullout tests were performed on shotcrete more than 28 days old. The presented results are within 0,68–1,10 MPa. A relatively poor bond strength of 0,3–0,4 MPa is otherwise often measured between shotcrete and the rock in the mine (Malmgren et al., 2005). The age dependent bond strength for the same type of shotcrete, but sprayed on concrete, have been investigated by Malmgren and Svensson (1999). Polynomial regression curves were later fitted to the results by Ansell (1999). The bond strength development between shotcrete and rock measured at temperatures of +7 °C and +20 °C are presented by Bryne et al. (2014). For this laboratory investigation, a specially developed test method was used (see also the following section). The shotcrete had a standard composition with a water-cement ratio of 0,45. The cement used is Swedish type “Anläggningscement” (CEM I 42.5 N – SR 3 MH/LA), which is a slower reacting cement for “civil engineering use”. A super-plasticiser was added to get a satisfying consistency and an alkali-free set accelerator was added in the nozzle during spraying, at 3–5% of the cement weight.

### *6.2 Mortar and concrete on rock or concrete*

For comparison are here also results from tests with mortar and concrete on rock or concrete given. A laboratory test method for measuring early bond strength was developed and described by Bryne et al. (2011) and Bryne & Ansell (2012). With the test setup, the shotcrete, first substituted with mortar, was

cast on concrete plates with predrilled cores that were pulled out from the plates while recording the pullout force, recalculated to bond strength. The first tests were with sprayable but cast cement mortar with composition comparable to standard shotcrete and with a water-cement ratio of 0,45. The cement is Swedish type “Byggcement” (cement for housing, CEM II/A-LL 42.5 R). In this initial phase, ordinary precast concrete plates was used to simulate hard rock surfaces. The quality of these was C25/30 and the surface in contact with the mortar was un-polished but fine-grained.

For the following laboratory investigation (Bryne et al., 2013), shotcrete was substituted with cast concrete, also with a composition comparable shotcrete, with a water-cement ratio of 0,45. However, in this case the cement is Swedish type “AnlÄggningscement” (cement for civil engineering use, CEM I 42.5 N - SR 3 MH/LA). For some of the tests a set-accelerator was added to the concrete mix. The concrete cores from the slabs were also replaced by granite cores. A comparison with the first tests using cement paste thus demonstrate the different rates of strength growth that is obtained with the two most common Swedish cement types.

### 6.3 Examples

The test results described in the previous two sections are compared in Figures 6.1–6.2. In the following, the mathematical expression for each curve is given for comparison, recalculated from the original references when needed so that the shotcrete age  $t$  is given in hours throughout. If not otherwise stated, the expressions are valid for ages up to at least 72 hours. The bond strengths  $f_{cb}$  is in MPa.

The bond strength development for shotcrete without set-accelerator but with Sodium silicate (water glass) of the type previously used in the Kiruna mine (Malmgren and Svensson, 1999 and Ansell, 1999) follows:

$$f_{cb} = -11,38 \cdot 10^{-12} t^4 + 2,12 \cdot 10^{-8} t^3 - 1,66 \cdot 10^{-5} t^2 + 6,08 \cdot 10^{-3} t + 2,84 \cdot 10^{-1} \quad (6.1)$$

For laboratory tested shotcrete on rock (Bryne et al., 2014), with “AnlÄggningscement” (CEM I 42.5 N - SR 3 MH/LA) and alkali-free accelerator, the bond strength development at +7 °C follows:

$$f_{cb} = 2,36 e^{-22,66/t^{1,03}} \quad (6.2)$$

For the same shotcrete tested at +20 °C the corresponding equation is:

$$f_{cb} = 1,55 e^{-43,95/t^{1,49}} \quad (6.3)$$

Initial tests with cement mortar cast on concrete (Bryne et al., 2011; Bryne & Ansell, 2012, Ahmed et al., 2012 and Ahmed & Ansell, 2012b) resulted in:

$$f_{cb} = 2,36 e^{-18,72/t^{0,97}} \quad (6.4)$$

while a follow-up test series (Bryne et al., 2013) using “Byggcement” (cement for housing, CEM II/A-LL 42.5R) for the mortar gave:

$$f_{cb} = 1,68 e^{-0,571/t^{1,230}} \quad \text{for } 0 \leq t \leq 24 \text{ hrs.} \quad (6.5)$$

Laboratory tests with concrete on granite cores, “AnlÄggningscement” (cement for civil engineering use, CEM I 42.5 N - SR 3 MH/LA) and without set-accelerator gave (Bryne et al., 2013):

$$f_{cb} = 1,30e^{-0,690/t^{1,250}} \tag{6.6}$$

With corresponding tests but with set-accelerator added resulted in:

$$f_{cb} = 3,64e^{-8,92/t^{0,45}} \tag{6.7}$$

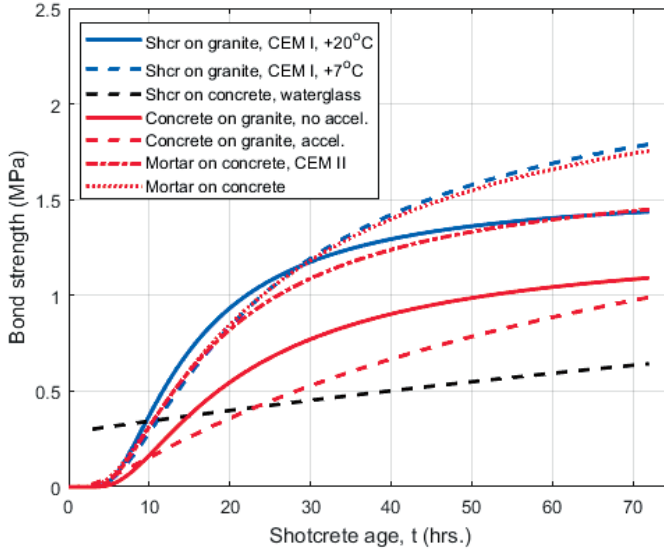


**Figure 6.1:** Bond strengths of shotcrete, concrete and mortar.

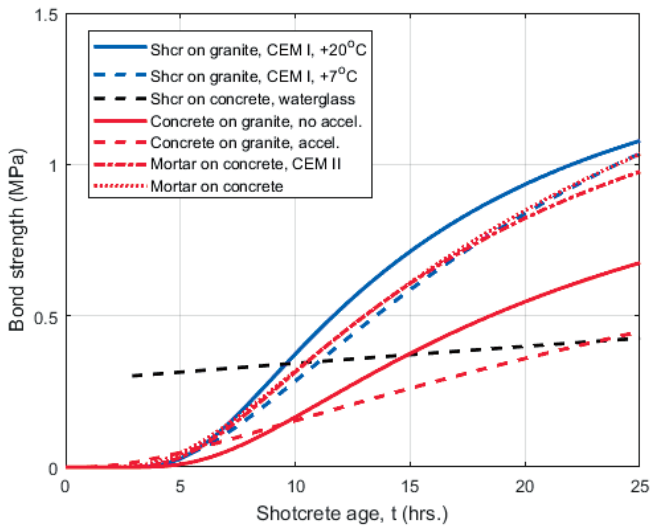


**Figure 6.2:** Bond strengths of shotcrete.



# Chapter 7

## Comparisons - previous and in situ results

In the following four sections, results calculated with the model presented in section 2 are compared with previous numerical results, measurements and observations in situ. The purpose is to verify the model and the modelling concept. Realistic and representative input data is used. However, it must be remembered that the model is restricted to describe vibrations over a relatively small area section with one-dimensional deformations in the direction orthogonal to this. For some of the cases studied, stress waves will reach the shotcrete in an oblique direction, and the results will therefore be an approximation to the resulting actions of normal- and shear stresses. Four cases, studied in the previous research are chosen as examples.

### *7.1 The Kiruna tests*

Results from tests with detonation of explosives in rock behind newly projected shotcrete are presented in detail by Ansell (1999) and Ansell (2004). The tests were conducted in the Kiruna mine where the rock type is iron ore with a density of 4800 kg/m<sup>3</sup> and with an estimated, relatively low modulus of elasticity of 40 GPa (see section 3.2 and Ansell, 2005, 2007a). The relationship between vibration velocity, distance and charge weight in the iron ore is given by case 12 in Table 4.1. The thickness variation of the shotcrete was not measured. However, the normal thickness of the Kiruna mine was at that time about 30 mm, as is assigned for the examples here. The density of the shotcrete was assumed to be 2100 kg/m<sup>3</sup>. The elastic modulus of the shotcrete is assumed to vary according to Eq. (5.5) and the bond between rock and shotcrete according to Eq. (6.1).

The damages in the form of ejected rock and shotcrete, as well as drum shotcrete sections with loss of bond to the rock, at the four test areas are summarized in Figures 7.1–7.4, where the calculated drum areas are also marked with red outlined rectangular areas. The calculation results are shown with 3D surfaces in Figure 7.5–7.8, where shotcrete age vs. distances for the respective test area's seven measurement points have also been marked, with “x” for points on the rock surface and “o” for points inside the rock. Table 7.1 summarizes damaged and undamaged sections for the four areas, which is the basis for the damage areas shown in Figures 7.1–7.4. The table also lists the dimensioning charge weights  $Q$  which have been calculated by considering the effect of long charges using Eq. (4.4), based on the measurement data provided by Ansell (1999). Here the distances at the central measurement points have been taken as mean values for the respective distance range.



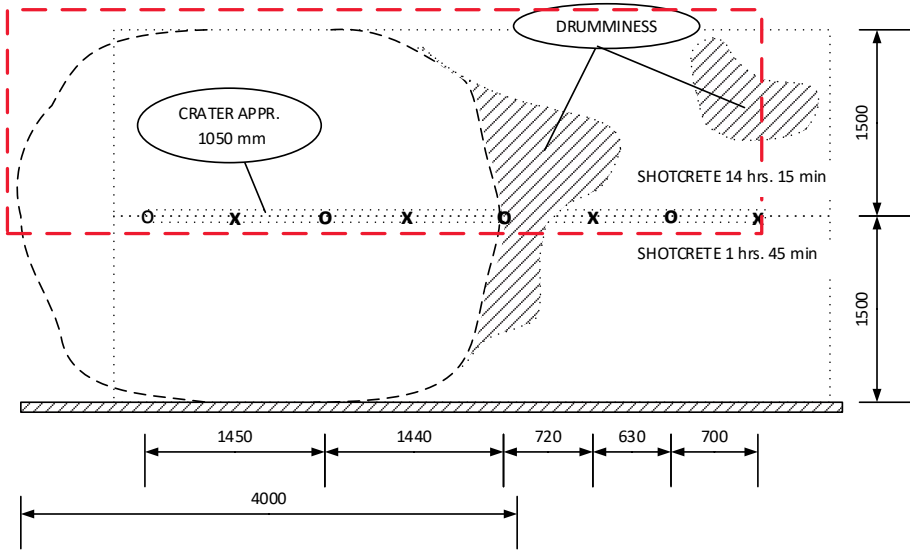


**Figure 7.1:** Result from Kiruna test area 1, from Ansell (1999). Area with calculated loss of shotcrete-rock bond is indicated with red lines (compare with Table 7.1).

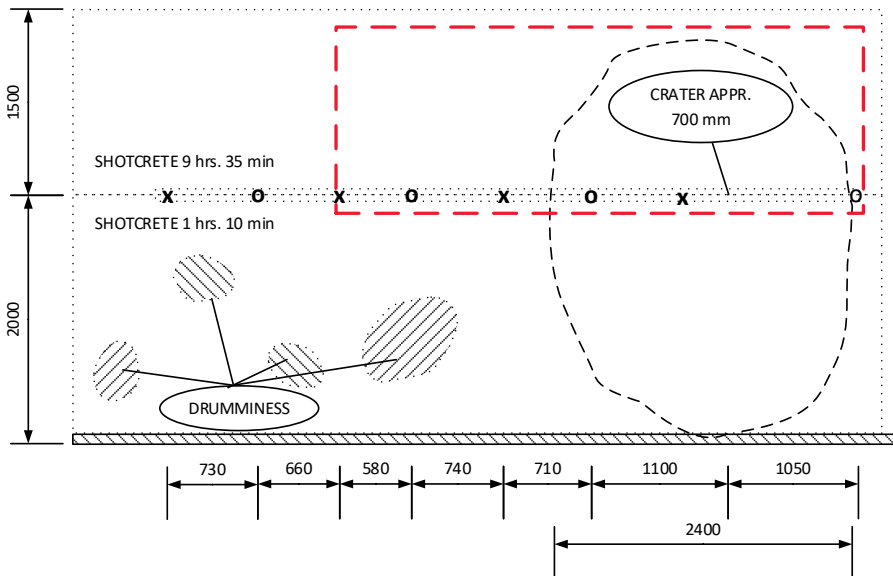


**Figure 7.2:** Result from Kiruna test area 2, from Ansell (1999). Area with calculated loss of shotcrete-rock bond is indicated with red lines (compare with Table 7.1).

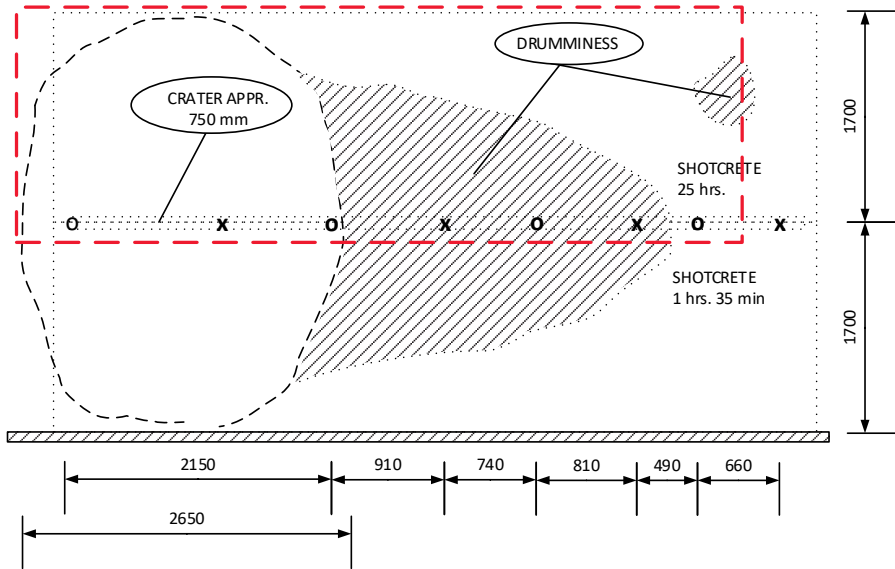


**Figure 7.3:** Result from Kiruna test area 3, from Ansell (1999). Area with calculated loss of shotcrete-rock bond is indicated with red lines (compare with Table 7.1).

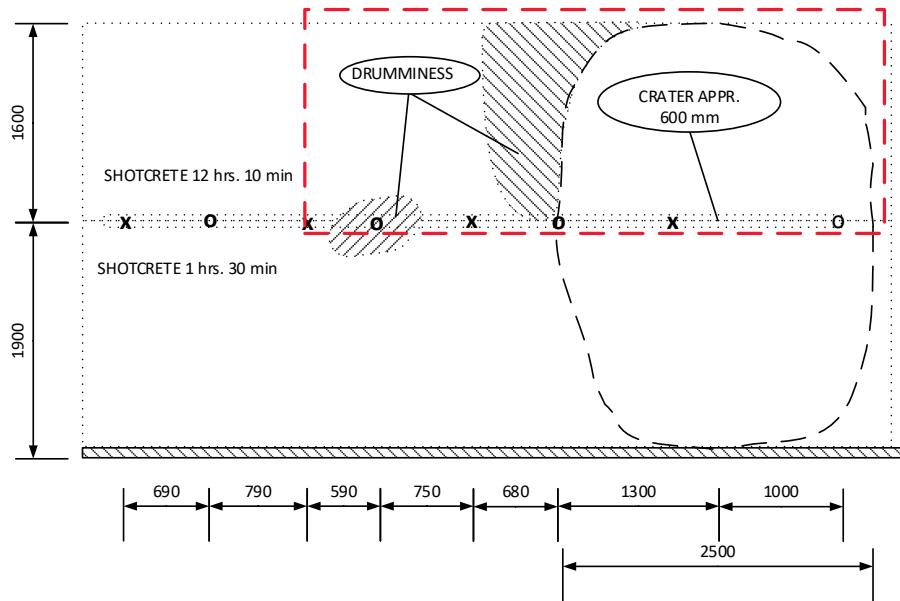


**Figure 7.4:** Result from Kiruna test area 3, from Ansell (1999). Area with calculated loss of shotcrete-rock bond is indicated with red lines (compare with Table 7.1).

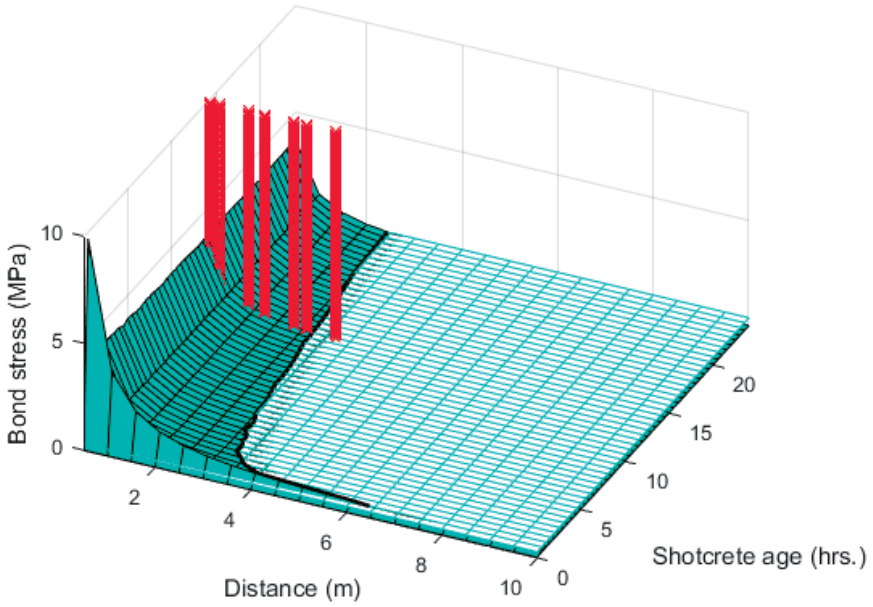


**Figure 7.5:** Calculated shotcrete-bond stresses for Kiruna test area 1. The red bars show results from the seven measurement points for 14 hrs old shotcrete and the damage limit curve is indicated.

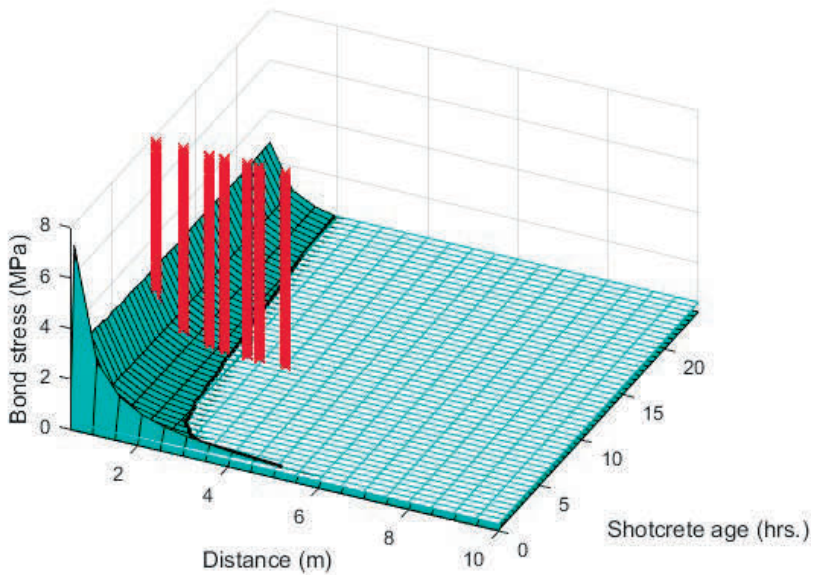


**Figure 7.6:** Calculated shotcrete-bond stresses for Kiruna test area 2. . The red bars show results from the seven measurement points for 9,5 hrs old shotcrete and the damage limit curve is indicated.

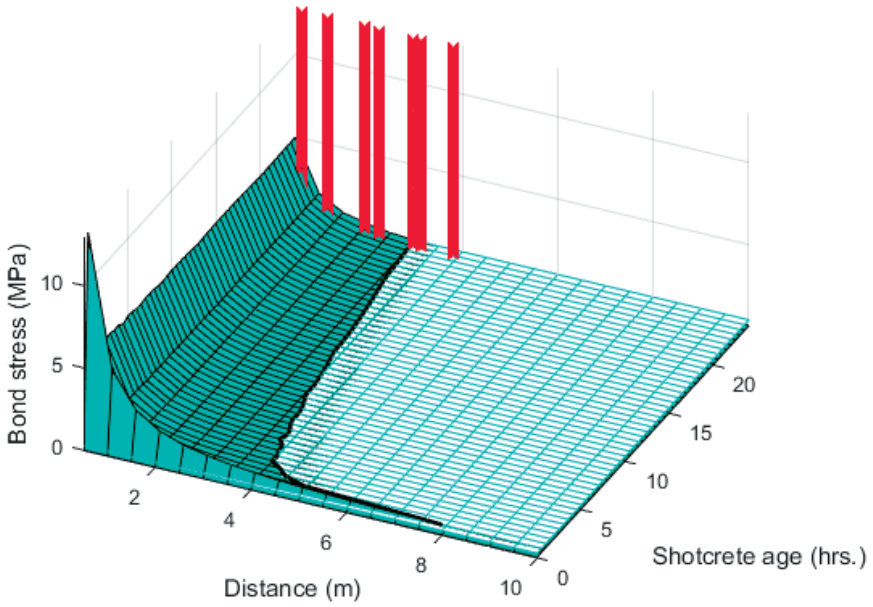


**Figure 7.7:** Calculated shotcrete-bond stresses for Kiruna test area 3. The red bars show results from the seven measurement points for 25 hrs old shotcrete and the damage limit curve is indicated.

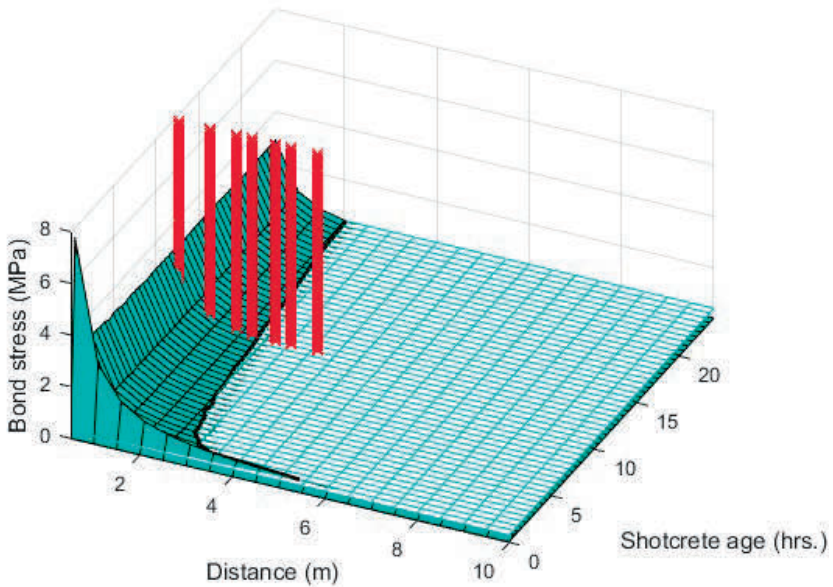


**Figure 7.8:** Calculated shotcrete-bond stresses for Kiruna test area 4. The red bars show results from the seven measurement points for 12 hrs old shotcrete and the damage limit curve are indicated.

**Table 7.1:** Summary of calculated shotcrete-bond failure for Kiruna test areas 1-4. The results are transferred to Figures 7.1-7.4.

Measurement point	1	2	3	4	5	6	7	$Q$ (kg)
Test 1	X	X	X	X	X	X	(x)	4,7
Test 2	X	X	X	X	(x)	-	-	3,0
Test 3	X	X	X	X	X	X	-	7,2
Test 4	X	X	X	X	(x)	-	-	3,3

X = Bond damage      (x) = Limit value for bond damage      - = Intact bond

## 7.2 The Södra länken tests

In situ measurements were carried out during tunnelling for the Södra länken road tunnels in Stockholm. The results are presented by Reidarman and Nyberg (2000), where the tests are described in detail, with the measurement points placed in the range of 5,2 m to 54,1 m distance between shotcrete and explosive charges. No shotcrete damage was observed during the measurements. A follow-up study with results analysed using finite element modelling has been conducted by Ahmed & Ansell (2014). The rock here has properties close to the normal Swedish bedrock, see Table 4.1 (case 5). The shotcrete is assumed to be 100 mm thick (Ahmed & Ansell, 2014), with a strength growth following the elastic modulus provided by Bryne (2014) and Eq. (5.12). The bond between rock and shotcrete is also believed to follow the results proposed by Bryne (2014), see Eq. (6.3).

For the tunnel blasting, a charge plan was used where each individual charge was  $Q=1,3$  kg (Ahmed & Ansell, 2014), for which calculated results are shown in Figure 7.9. The test report (Reidarman and Nyberg, 2000) mentions that a combined effective charge weight should have been  $Q=8,6$  kg, for which alternative calculation results are shown in Figure 7.10. The figures show the geometric positions of the three measurement and observation points with the shortest distance to the charges, i.e. 5,2; 6,3 and 9,8 m. During the in situ measurements, the shotcrete had reached a fully hardened state, why the points in Figures 7.9 and 7.10 have been placed at the lowest possible shotcrete ages, where the calculations indicate that blasting could have occurred without causing damage, i.e. at 14 and 40 hours of shotcrete age. As a guideline for safe blasting, a minimum compressive shotcrete strength of 6 MPa and a maximum permitted vibration velocity of 150 mm/s was allowed (Reidarman and Nyberg, 2000). According to Eq. (4.2) and Table 4.1, this corresponds to the two cases of distance  $R$  which is 3,4 m and 8,8 m, respectively. The development of the shotcrete elastic modulus is assumed to be based on the following compressive strength development (Bryne, 2014):

$$f_{cc} = 30,8e^{-661,61/t^{2,17}} \quad (\text{MPa}) \quad (7.1)$$

A calculation gives 6 MPa compressive strength after 16 hours. These limit values are indicated by blue lines in the figures, where it appears that these are set on the safe side relative to the calculations. However, Figure 7.10 shows that, under these limit values, it would never be possible for the shotcrete to remain undamaged at 5,2 m and 6,3 m distance if the charge was 8,6 kg. It should also be noted here

that the shotcrete would theoretically, according to the calculations, be able to withstand the explosions already during the early short age range of 3–4 hours.

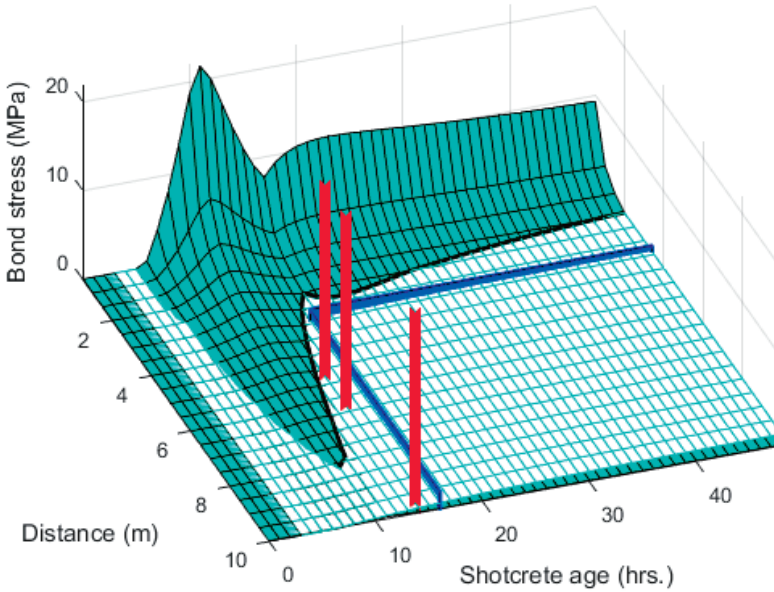


**Figure 7.9:** Calculated shotcrete-bond stresses from a single charge in the Södra länken tunnel. Three measurement points (red) for 14 hrs old shotcrete, blast restriction (blue) and calculated damage limit curve are indicated.

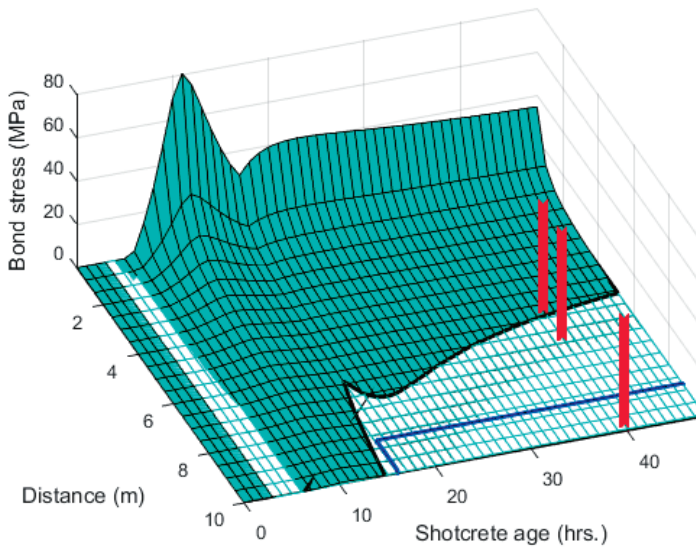


**Figure 7.10:** Calculated shotcrete-bond stresses from a multiple charges in the Södra länken tunnel. Three measurement points (red) for 40 hrs old shotcrete, blast restriction (blue) and calculated damage limit curve are indicated.

### 7.3 Previous numerical results

The previously presented calculation results (Ansell, 2005 & 2007a) shown in Figures 2.2 and 2.3 are reproduced here with the model calculation results for the three shotcrete thicknesses 25, 50 and 100 mm in Figures 7.11–7.13. For the three cases the explosive weights are  $Q=2$  kg while shotcrete age and distance  $R$  to the charge have been varied. The six curves from Figures 2.2 and 2.3 are seen as corresponding red and blue curves on the results. Note that in Figure 2.2, results are shown for 28 days old shotcrete, which here has been transposed to the age of 22 hours. This approximation is made for clarity in the figure and motivated since the black curve has converged towards the value it also have at 28 days of shotcrete age. Also, the 3D surface corresponding to the bond strength for clarity have been omitted in Figures 7.11 and 7.12, but with the limiting curves from the intersections between the strength and loading surfaces are still shown with black solid lines. The elastic modulus of the shotcrete follows the relation given by Eq. (5.4), the bond is given by Eq. (6.1) and the relation between vibration velocity - charge weight - distances by Table 4.1 (case1).

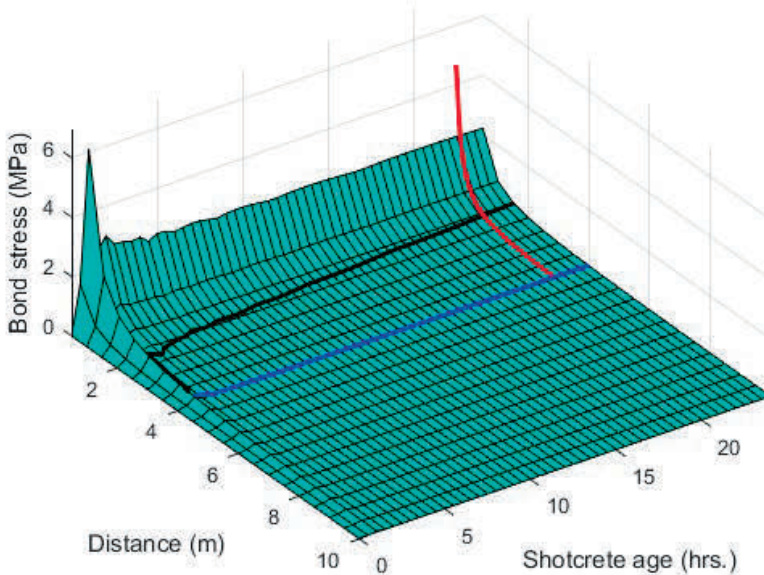


**Figure 7.11:** Calculated shotcrete-bond stresses from a 2 kg charge for 25 mm thick shotcrete, in comparison with previous analytical results (see Figures 2.2-2.3).

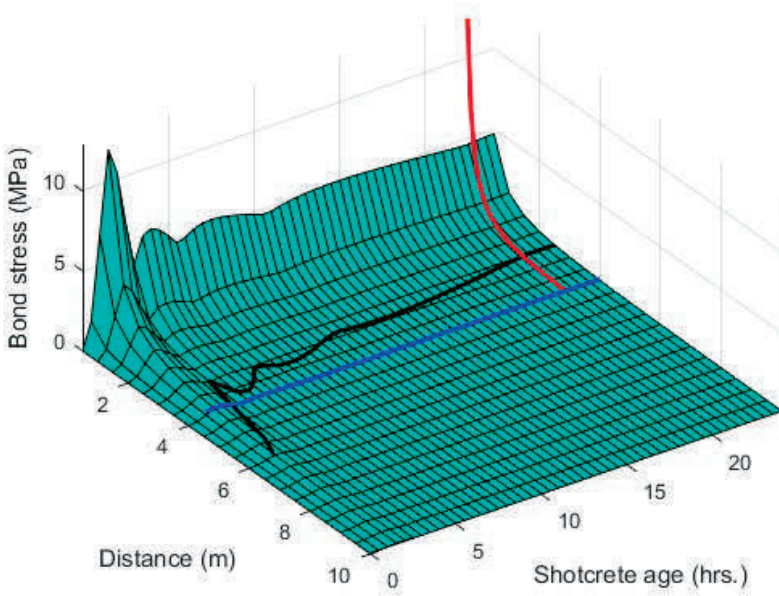


**Figure 7.12:** Calculated shotcrete-bond stresses from a 2 kg charge for 50 mm thick shotcrete, in comparison with previous analytical results (see Figures 2.2-2.3).

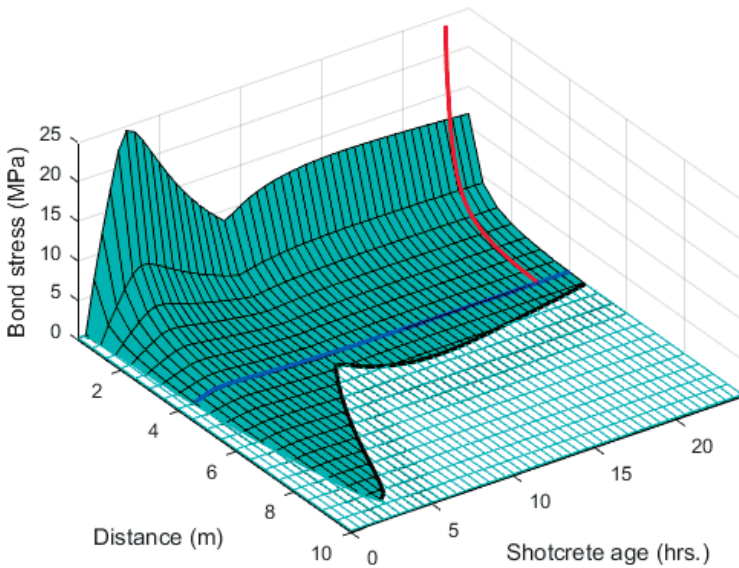


**Figure 7.13:** Calculated shotcrete-bond stresses from a 2 kg charge for 100 mm thick shotcrete, in comparison with previous analytical results (see Figures 2.2-2.3).



## 7.4 Large scale blasting

The previous examples show good compliance for relatively small charge weights at shorter intervals. This is the case in tunnelling where a large number of smaller charges are detonated in sequence to achieve minimal damage to surrounding rock and to produce a tunnel geometry as close as possible to the prescribed one. In mining operations, the purpose is instead to fracture large volumes of rock with powerful explosions. An example is shown in Figure 7.14, illustrating the principle of sublevel caving in the Kiruna mine (Ansell, 2007b). Here, an  $L_c = 20$  m long charge can contain  $Q=220$  kg of explosives detonated in sequence with other charges of up to a total of 2000 kg. During such operations, a shotcrete damage limit of approximately 9 m ( $x$  in the figure) has been observed, for “hardened” shotcrete.

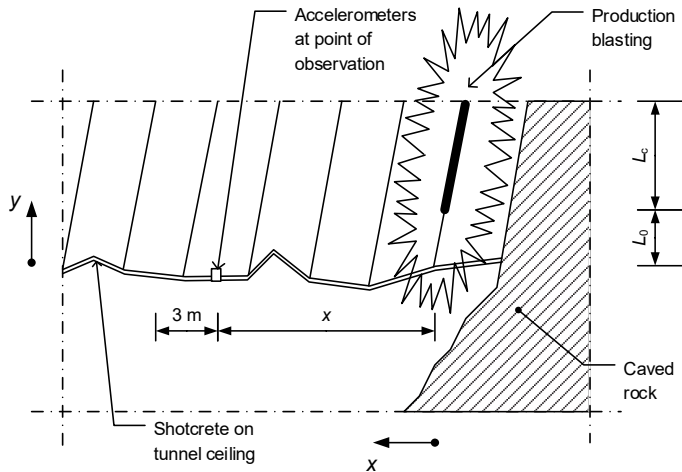


**Figure 7.14:** Production blasting at tunnel front in Kiruna. Tunnel ceiling with shotcrete support and one measurement point at  $x$ . From Ansell (2007b).

When such a large amount of explosives is detonated it is important that reduction of the charge weight  $Q$  is performed with respect to the geometry and length of the charge, according to Eqs. (4.3-4.4). The geometry shown in Figure 7.14, typically with  $L_0 = 4$  m and  $L_c = 20$  m, leads to dispersion of blasting energy, in time and space, before it reaches the shotcrete. Following Eq. (4.4) and assuming that the distance  $R$  here is taken as the length from the bottom of the charge to a point of observation,  $R = 9,8$  m and  $L_c = 20$  m gives a length reduction factor of  $f = 0,78$  and an effective charge weight of  $Q = 172$  kg. Numerical results based on this and an assumed shotcrete thickness of 50 mm in the Kiruna mine are presented in Figures 7.14-15. The rock and shotcrete material properties are here the same as used in the examples of section 7.1. In Figure 7.14 it can be seen that the limit curve converges towards  $R = 10$  m for increasing shotcrete ages. This is confirmed by the results as seen in Figure 7.15, in this case with a comparison to results calculated with the unadjusted amount of explosives, i.e.  $Q = 220$  kg. The figure also shows that  $Q = 145$  kg ( $f = 0,66$ ) would have given exactly the observed damage level of  $R = 9,8$  m (i.e.  $x = 9$  m). This factor would however correspond to  $R = 6,8$  m and  $x = 5,5$  m in Eq. (4.4).

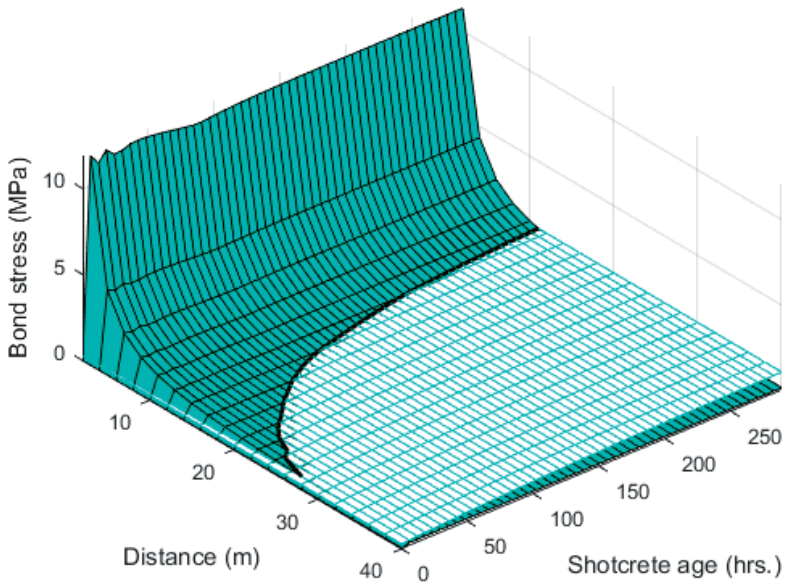


**Figure 7.15:** Calculated shotcrete-bond stresses from an effective charge of 172 kg (un-adjusted 220 kg) in the Kiruna mine. Calculations for long distances and long-time (576 hrs = 24 days).

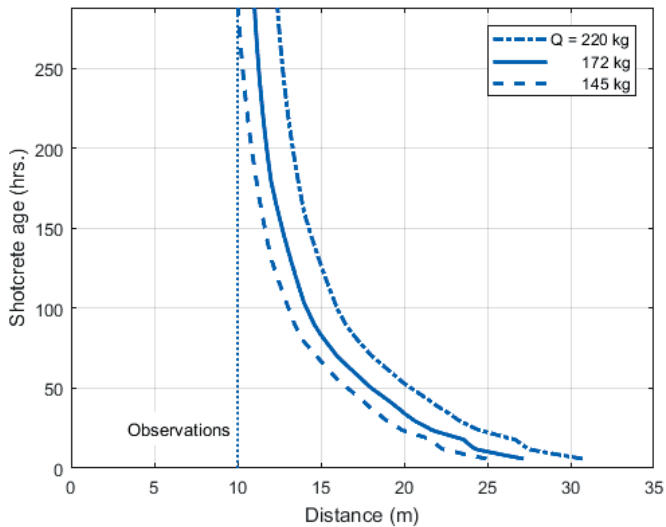


**Figure 7.16:** Comparison between limit-lines from results calculated for effective charges of 220, 172 and 145 kg in the Kiruna mine. Calculations for long distances and long-time (576 hrs = 24 days).



## Chapter 8

# Conclusions and recommendations

The previously developed and tested numerical analysis method, that is based on a dynamic spring-mass model, has here proven to be highly computationally effective and to give results that show good agreement with previous results, in situ measurements and observations. Through relatively short calculation times it has been possible to perform analysis for and evaluate a large number of combinations of input parameters. The suggested guidelines graphically presented in Appendix B are based on a series of 691 200 unique calculations using the numerical model. The limit curves included in the guidelines have been stored numerically in a database and contain, in addition to the reported conditions between distances and shotcrete ages, the corresponding stress levels at the rock-shotcrete interface. This is illustrated in the presented examples where such results are displayed as 3D plots.

As input parameters for the rock properties, summaries of typical values for Swedish rock conditions are presented. These cover density, wave propagation velocity, elasticity modulus and for comparison also compressive strength, which however is not used by the numerical calculation model. The character of the rock is also represented by characteristic distances between fractures and imperfections. These distances may, for example, correspond to the EDZ (excavation damage zone) in a tunnel. The crack distance and the wave propagation velocity are in the model used to calculate a characteristic frequency for the stress wave that propagates from the detonation point, through the rock and towards the shotcrete.

The magnitude of the incoming stress waves is determined from the particle vibration velocities which can be calculated as function of charge weight and distance. The scaling laws used for this also provide a description of the nature and characteristics of the rock. The equations are often based on in situ measurements, and the report shows a compilation of typical representative values for Swedish bedrock, granite and gneiss. Since several investigations have been carried out in Swedish mines, for example in Kiruna, are also data representative for iron ore included to facilitate comparisons. The guidelines presented are thus also useful under some mining conditions.

Before the project was initiated, it was known that representative and reliable material data for young and hardening shotcrete is scarce. This was confirmed by the extensive literature search that has been conducted. An important element in the collection of material data has been to review, compile, compare and evaluate the data that has provided the basis for previous research within the field. One important governing parameter during the calculations is the development of the modulus of elasticity with increasing shotcrete age. There are basically no representative data from in situ measurements on young shotcrete. Often, conversions to elastic modulus are done based on measured compressive strength. However, these relations are not fully verified, and relatively commonly are equations for cast concrete used, which may only be considered as approximations. In the compilation, however, results are

included from laboratory tests where the compressive strength has been accurately measured for very young shotcrete, after which each calculated modulus of elasticity have been used and evaluated in follow-up numerical calculations.

The limit values presented here as practical guidelines have been developed by finding intersections between 3D surfaces representing shotcrete age-distance-bond stresses, for stresses arising from blasting and for bond strengths between rock and shotcrete. For this strength, very little is documented when it comes to young and hardening shotcrete. As a basis for the calculations, are here results from an important laboratory investigation with shotcreted specimens used. The results are compared with the corresponding tests performed on mortar and cast concrete, on granite and on concrete substrates.

The calculation method has been verified through presented examples where the calculated results are compared with previously published calculation results and in situ measurements and observations. Good agreement is given in all cases. First, it is demonstrated how the calculation model can be applied to reflect the conditions that existed during an extensive test series conducted in the Kiruna mine. Observed zones with bond losses after testing are compared with calculated results for respective measurement points, and it is evaluated if this is below or above the limit for shotcrete damage according to the calculation model. The second round of examples includes a comparison with observations and vibration in situ measurements during tunnelling for the Södra Länken in Stockholm. Here, the results are also compared with the guidelines used for those jobs. It is evident that these older, empirically established limit values relatively accurate, but also that they have been conservative and perhaps non-consistent. In previously published research papers, calculation results from the same model as in this project have been put forth, but only for some combinations of input data. In a third set of examples, some of these previous results are compared with corresponding ones obtained with the current calculation method. The fourth and last examples show a comparison with in situ observations during large-scale mining blasting in the Kiruna mine. Even with the considerably higher charge weights at longer distances, there is relatively good correspondence between observations and calculated results.

Recommended limit values for practical use are given graphically in the report appendix. The large amount of data that has to be displayed causes the variation in the input parameters to be limited. As representative rock types, ten combinations of rock properties have been selected based on the summaries that have been made and discussed. These typically include granite-type Swedish bedrock and heavier iron ore, of the type found in the Kiruna mine. The latter has been included to facilitate comparisons with previous results, but may also provide guidelines for blasting in mining. The properties selected for granite correspond to the lower and upper limits often indicated for its density and wave propagation velocity, and also for representative scaling between vibration velocity, charge weight and distance. The elastic properties of young and hardening shotcrete are represented here by previously published and, in many cases, discussed results for a high and a low-strength shotcrete type and from results established through laboratory testing. The development of the bond strength between shotcrete and rock is here represented by a case with one higher and one with a lower final strength.

For the future work, focus should be on obtaining more material data representative for young and hardened shotcrete under in situ conditions. More large-scale investigations with observations of damage and vibration measurement should also be performed. These results should then be accurately compared to the recommended limit values presented here, in order to evaluate the level of safety these provide and if they are less representative under certain conditions than others. Continuous practical use of the guidelines and feedback of results from comparison between recommended and observed limits for damage are important for future upgrades of the method, result database and recommendations.

# Bibliography

Ahmed L, Ansell A. (2012a). "Structural dynamic and stress wave models for analysis of shotcrete on rock exposed to blasting". *Engineering structures*, 35, 11-17.

Ahmed A, Ansell A. (2012b). "Laboratory investigation of stress waves in young shotcrete on rock". *Magazine of Concrete Research*, 64, 899-908.

Ahmed L, Ansell A. (2014). "Vibration vulnerability of shotcrete on tunnel walls during construction blasting". *Tunnelling and Underground Space Technology*, 42, 105-111.

Ahmed L, Malm R, Ansell A. (2012). "Finite element simulation of shotcrete exposed to underground explosions". *Nordic Concrete Research*, 45, 59-74.

Ansell A. (1999). *Dynamically loaded rock reinforcement*, Doctoral thesis, KTH Royal Institute of Technology, Trita-BKN. Bulletin 52, Stockholm.

Ansell A. (2004). "In situ testing of young shotcrete subjected to vibrations from blasting". *Tunnelling and Underground Space Technology*, 19, 587-596.

Ansell A. (2005). "Recommendations for shotcrete on rock subjected to blasting vibrations, based on finite element dynamic analysis". *Magazine of Concrete Research*, 57, 123-133.

Ansell A. (2007a). "Dynamic finite element analysis of young shotcrete in rock tunnels". *ACI Structural Journal*, 104, 84-92.

Ansell A. (2007b). "Shotcrete on rock exposed to large-scale blasting". *Magazine of Concrete Research*, 59, 663-671.

Ansell A, Silfwerbrand J. (2003). "The vibration resistance of young and early age concrete". *Structural Concrete*, 4, 125-134.

Bieniawski Z. (1978). "Determining rock mass deformability: Experience from case histories". *International Journal of Rock Mechanics and Mining Sciences and Geomechanics Abstracts*, 15, 237-247.

Bodare A. (1997). *Jord- och bergdynamik*. Inst. för Anläggning och Miljö, KTH, Stockholm (In Swedish).

Bryne LE, Ansell A. (2012). "Laboratory testing of the bond strength between shotcrete and rock". In: *Symposium - Concrete Structures for Sustainable Community*, Stockholm, 433-436.

Bryne LE, Ansell A. (2013). "Laboratory testing of early age bond strength between concrete for shotcrete use and rock". *Nordic Concrete Research*, 47, 81-100.

Bryne LE, Ansell A, Holmgren J. (2014). "Laboratory testing of early age bond strength of shotcrete on hard rock". *Tunnelling and Underground Space Technology*, 41, 113-119.

Bryne LE, Holmgren J, Ansell A. (2011). "Experimental investigation of the bond strength between rock and hardening sprayed concrete". In: *Sprayed concrete - Modern use of wet mix sprayed concrete for underground support. Sixth international conference on sprayed concrete*, Tromsø, 77-88.

Byfors J. (1980). *Plain concrete at early ages*. Research Fo 3:80, CBI, Stockholm.

BYGG 1A. (1971). *Handboken för hus-, väg- och vattenbyggnad, Huvuddel 1A*. AB Byggmästarens förlag, Stockholm (In Swedish).

BYGG 1B. (1971). *Handboken för hus-, väg- och vattenbyggnad, Huvuddel 1B*, AB Byggmästarens förlag, Stockholm (In Swedish).

BYGG T. (1990). *Handboken Bygg – Byggtabeller*. LiberFörlag, Stockholm (In Swedish).

CEB-FIP. (1991). *Model Code 1990, Chapters 1—3*, Final Draft, Bulletin D'Information No. 203, Comite Euro-International du Beton (CEB), Vienna.

Chang Y. (1994). *Tunnel support with shotcrete in weak rock - a rock mechanics study*. Doctoral thesis, Div. Soil and Rock Mechanics, Royal Institute of Technology, Stockholm.

Clough RW, Penzien J. (1993). *Dynamics of structures*. 2nd ed. McGraw-Hill, New York.

Dowding CH. (1996). *Construction vibrations*. Prentice Hall, Upper Saddle River.

Hahn T. (1983). *Sprubetonns vidhäftning mot olika bergtyper*. BeFo 55:1/83, Stiftelsen Bergteknisk Forskning - BeFo och Fortifikationsförvaltningen, Stockholm (In Swedish).

Hahn T, Holmgren J. (1979). "Adhesion of shotcrete to various types of rock surfaces and its influence on the strengthening function of shotcrete when applied on hard jointed rock". In: *International Society for Rock Mechanics, 4th International Conference*, Montreux.

Holmberg R, Persson PA. (1980). "Design of tunnel perimeter blasthole patterns to prevent rock damage". *Trans Inst Mining and Metallurgy*, Vol. A, 37-70.

James G. (1998). *Modelling of young shotcrete on rock subjected to shock wave*. Master thesis, KTH Structural Engineering, Stockholm.

Jinnerot M, Nilsson H. (1998). *Experimentell studie av stötvågsutbredning och skadezonsberäkning vid ortdrivning*. Master thesis, Inst. för Geoteknik, Chalmers, Gothenburg (In Swedish).

Lagerblad B, Holmgren J, Fjällberg L, Vogt C. (2006). *Hydratation och krympning hos sprubetong*. SveBeFo Report K24, Stockholm (In Swedish).

Lundborg N, Holmberg R, Persson PA. (1978). *Markvibrationers avstånds- och laddnings-beroende*. Rapport R11:1978, Statens råd för byggnadsforskning, Stockholm (In Swedish).

Malmberg B. (1992). *Guidelines and recommendations - a compilation*. Draft document for the ITA WG shotcrete use, Stockholm.

Malmgren L. (2001). *Shotcrete rock support exposed to varying load conditions*. Licentiate thesis, Dept. of Civil and Mining Engineering, Division of Rock Mechanics, Luleå University of Technology, Luleå.

Malmgren L, Nordlund E, Rolund S. (2005). "Adhesion strength and shrinkage of shotcrete". *Tunnelling and Underground Space Technology*, 20, 33-48.

- Malmgren L, Svensson T. (1999). "Investigation of important parameters for unreinforced shotcrete as rock support in the Kiirunavaara mine, Sweden". In: *Proceedings of the 37th U.S. Rock Mechanics Symposium*, Vail, 629-635.
- Meschke G, Kropik C, Mang HA. (1996). "Numerical analyses of tunnel linings by means of a viscoplastic material model for shotcrete". *Int. j. numer. methods eng.*, 39, 3145-3162.
- Neuner M, Schreter M, Unteregger D, Hofstetter G. Influence of the Constitutive Model for Shotcrete on the Predicted Structural Behavior of the Shotcrete Shell of a Deep Tunnel. *Materials*, 10, 577, 2017.
- Nilsson C. (2009). *Modelling of dynamically loaded shotcrete*. Master thesis, KTH Concrete Structures, Stockholm.
- Nyberg U, Fjellborg S. (2000). "Controlled drifting and estimation of blast damage". In: *Explosives & Blasting Techniques*, Balkema, Rotterdam, 207-216.
- Oreste PO, Peila D. (1997). "Modelling progressive hardening of shotcrete in convergence-confinement approach to tunnel design". *Tunnelling and Underground Space Technology*, 12, 425-431.
- Ouchterlony F, Sjöberg C, Jonsson BA. (1993). "Blast damage predictions from vibration measurements at the SKB underground laboratories at Äspö in Sweden". In: *Proceedings of the ninth annual symposium on explosives and blasting research*, San Diego, 189-197.
- Persson PA. (1997). "The relationship between strain energy, rock damage, fragmentation, and throw in rock blasting". *Fragblast – International Journal of Blasting and Fragmentation*, 1, 99-110.
- Pöttler R. (1990). "Time-dependent rock - shotcrete interaction". *Computers and geotechnics*, 9, 149-169.
- Reidarman L, Nyberg U. (2000). *Vibrationer bakom front vid tunneldrivning i Södra Länken - Betydelse för nysprutad betong?* SveBeFo-Report 51, Rock Engineering Research Foundation, Stockholm (In Swedish).
- Stille H, Nord G. (1990). *Bergmekanik, del 1*. Inst. för Jord- och Bergmekanik, KTH, Stockholm (In Swedish).
- Vandewalle M. (1996). "Early fiber reinforced shotcrete strength". In: *Second international symposium on Sprayed Concrete*, Gol, 313-315.





# Appendix A

## Input data

Guidelines for safe limits, with respect to distance and shotcrete age, is given for various conditions in Appendix B. In the following are the input data for these conditions given, organized under headlines for *Rock types*, *Shotcrete types* and *Bond types*.

### *Rock types*

The ten rock types covered in the guidelines are defined in Table A.1. These represent typical Swedish bedrock of granite type and heavier iron ore, to facilitate comparison with observations from the mines in northern Sweden.

**Table A.1:** *Rock types covered in the guidelines (Appendix B), with  $v_{\max} = v_1 \cdot (R / \sqrt{Q})^{-b}$  (mm/s).*

Rock type	$c$ (m/s)	$\rho$ (kg/m <sup>3</sup> )	$H$ (m)	$f$ (Hz)	$v_1$ (mm/s)	$b$	Comments
1	3500	2500	0,50	1750	700	1,5	Bedrock (granite)
2	3500	2500	0,50	1750	1000	1,5	- softer type
3	3500	2500	0,25	3500	700	1,5	Bedrock (granite)
4	3500	2500	0,25	3500	1000	1,5	- softer type
5 <sup>a</sup>	7000	2800	0,50	3500 <sup>a</sup>	700	1,5	Bedrock (granite)
6 <sup>b</sup>	7000	2800	0,50	3500 <sup>b</sup>	1000	1,5	- harder type
7	7000	2800	0,25	7000	700	1,5	Bedrock (granite)
8	7000	2800	0,25	7000	1000	1,5	- harder type
9	6300	4800	0,50	3150	830	1,4	Iron ore (magnetite)
10	6300	4800	0,25	6300	830	1,4	Iron ore (magnetite)

<sup>a</sup> Same  $f$  as type 3. Results presented together in Appendix B.

<sup>b</sup> Same  $f$  as type 4. Results presented together in Appendix B.

Apart from the density  $\rho$ , the stress wave propagation velocity  $c$  and typical distance between imperfections and cracks  $H$ . The latter two gives the characteristic frequency  $f$  of a stress wave through the rock. It should be noted in Table A.1 that Rock types 3/4 and 5/6 have identical  $f$  which gives the same numerical results in the numerical analyses. Guidelines for these cases are therefore grouped together in Appendix B.

Parameters  $v_1$  and  $b$  for calculating peak particle velocities (ppv)  $v_{\max}$  are also given.

### Shotcrete types

All shotcrete types are here assumed to have a density of  $2100 \text{ kg/m}^3$ .

Three types of shotcrete with characteristically different developments of the elastic modulus are used as input, as seen in Figure A.1. Below the equations corresponding to the curves are given, with their original equation numbers from the project report. The shotcrete age  $t$  is in hours and the elastic modulus  $E$  in GPa.

$$\text{Shotcrete type 1: } E = 21,2e^{-3,00/t^{0,60}} \quad (5.8)$$

$$\text{Shotcrete type 2: } E = 28,7e^{-4,12/t^{0,70}} \quad (5.2)$$

$$\text{Shotcrete type 3: } E = 30,2e^{-397,0/t^{2,17}} \quad (5.12)$$

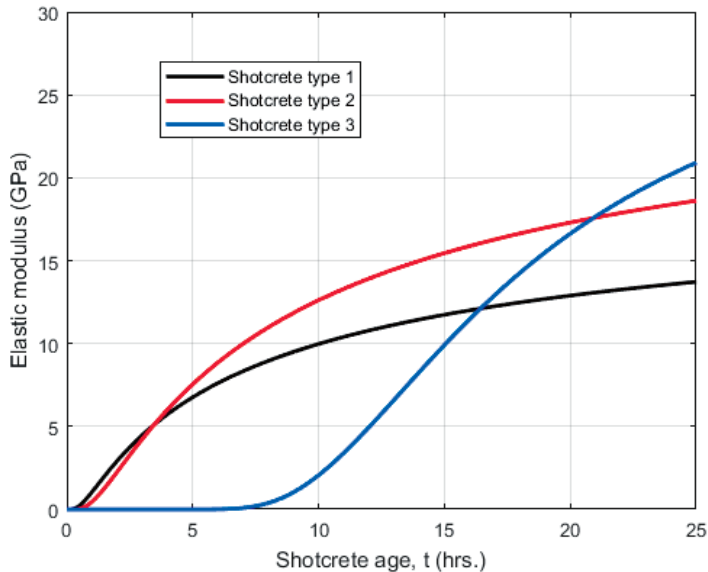


**Figure A.1:** Elastic moduli of shotcrete types covered in the guidelines (Appendix B).

### ***Bond types***

Two types of development of the bond between shotcrete and rock is chosen as input, see Figure A.2.

It should be noted that Bond type 1 originates from testing of cast concrete on granite.

Below the equations corresponding to the curves are given, with their original equation numbers from the project report. The shotcrete age  $t$  is in hours and the bond strength  $f_{bd}$  in MPa.

$$\text{Bond type 1:} \quad f_{cb} = 3,64e^{-8,92/t^{0,45}} \quad (6.7)$$

$$\text{Bond type 2:} \quad f_{cb} = 1,55e^{-43,95/t^{1,49}} \quad (6.3)$$

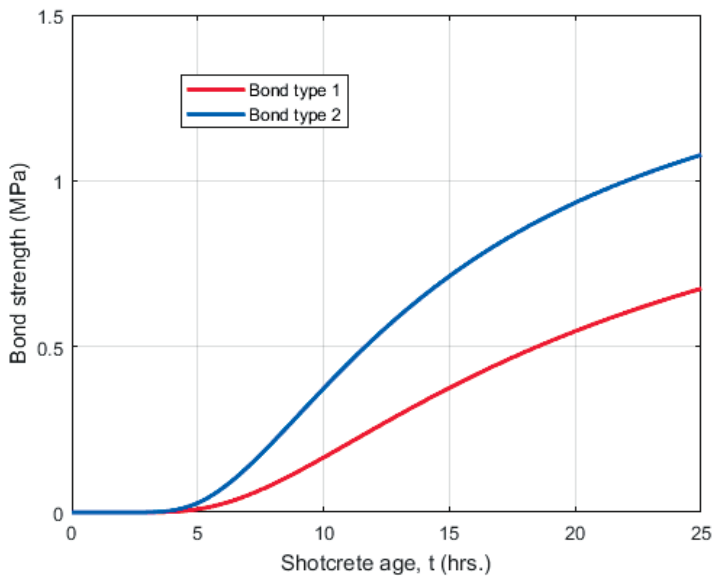


**Figure A.2:** Bond strengths of shotcrete types covered in the guidelines (Appendix B).



# Appendix B

## Recommended vibration limits

Here are guidelines for safe limits, with respect to distance and shotcrete age, given for the various conditions defined in Appendix A.

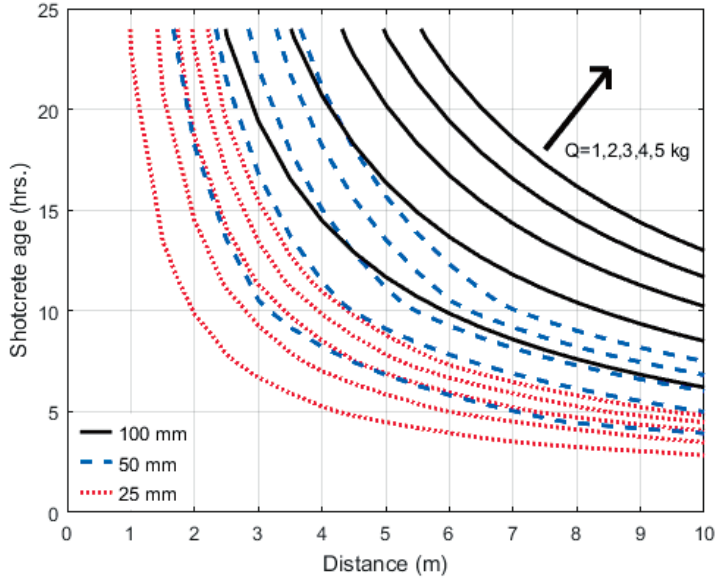
The guidelines are given as a series of diagrams organized after rock type. Each figure contain 15 curves, representing the limits for 25, 50 and 100 mm thick shotcrete exposed to detonation of 1, 2, 3, 4 or 5 kg of explosives.

It should be noted that in some figures some curves may be outside the range shown. As standard, distances up to 10 m and shotcrete ages up to 24 hrs. are included, but for the later figures these ranges are doubled.

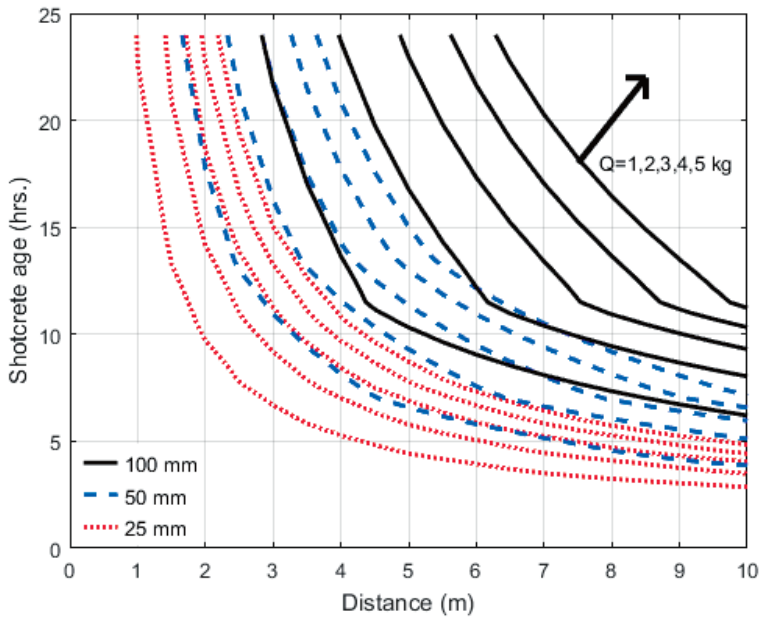
For each Rock type, there are six figures each corresponding to one combination of the three shotcrete types and two bond types, as summarized in the following:

Rock type 1	Bedrock (Granite)	Figures B.1 – B.6	pages 48 - 50
Rock type 2		Figures B.7 – B.12	pages 51 - 53
Rock type 3/5		Figures B.13 – B.18	pages 54 - 56
Rock type 4/6		Figures B.19 – B.24	pages 57 - 59
Rock type 7		Figures B.25 – B.30	pages 60 - 62
Rock type 8		Figures B.31 – B.36	pages 63 - 65
Rock type 9	Iron ore (Magnetite)	Figures B.37 – B.42	pages 66 - 68
Rock type 10		Figures B.43 – B.48	pages 69 - 71

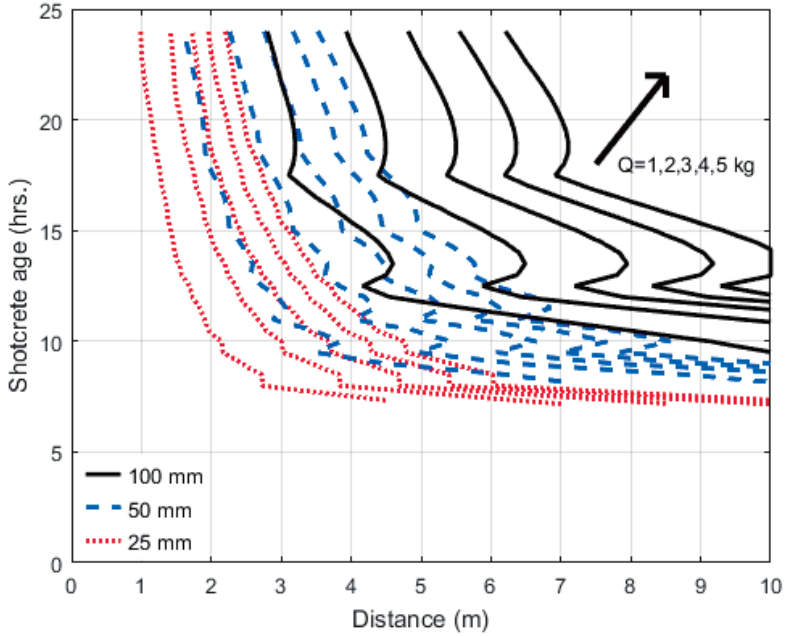
*Rock type 1*



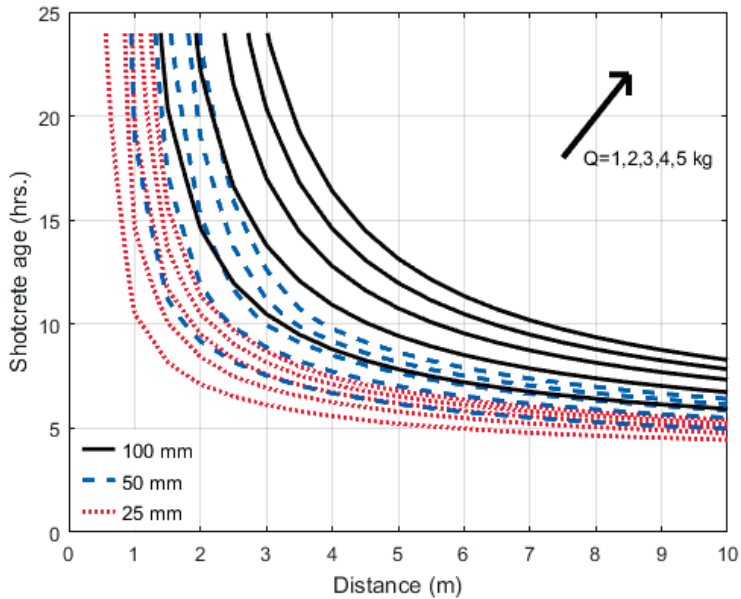
**Figure B.1:** Shotcrete type 1, Bond type 1, Rock type 1 ( $H = 0,50\text{ m}$ ,  $v_1 = 700\text{ mm/s}$ ,  $f = 1750\text{ Hz}$ ).



**Figure B.2:** Shotcrete type 2, Bond type 1, Rock type 1 ( $H = 0,50\text{ m}$ ,  $v_1 = 700\text{ mm/s}$ ,  $f = 1750\text{ Hz}$ )

*Rock type 1*

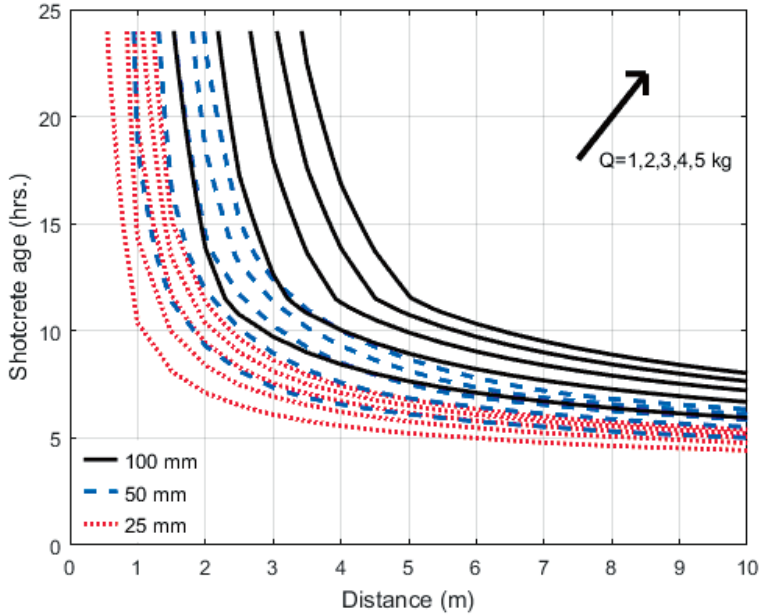
**Figure B.3:** Shotcrete type 3, Bond type 1, Rock type 1 ( $H = 0,50$  m,  $v_1 = 700$  mm/s,  $f = 1750$  Hz).



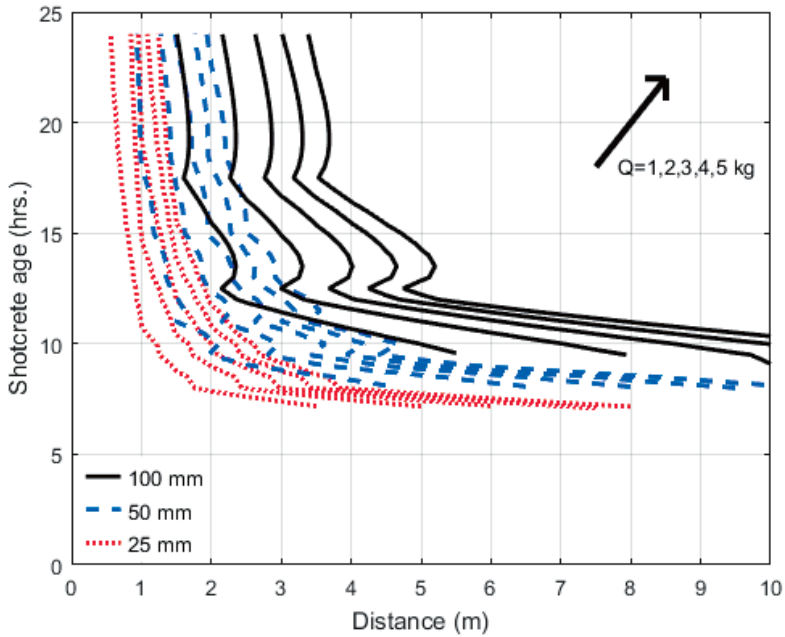
**Figure B.4:** Shotcrete type 1, Bond type 2, Rock type 1 ( $H = 0,50$  m,  $v_1 = 700$  mm/s,  $f = 1750$  Hz).



*Rock type 1*

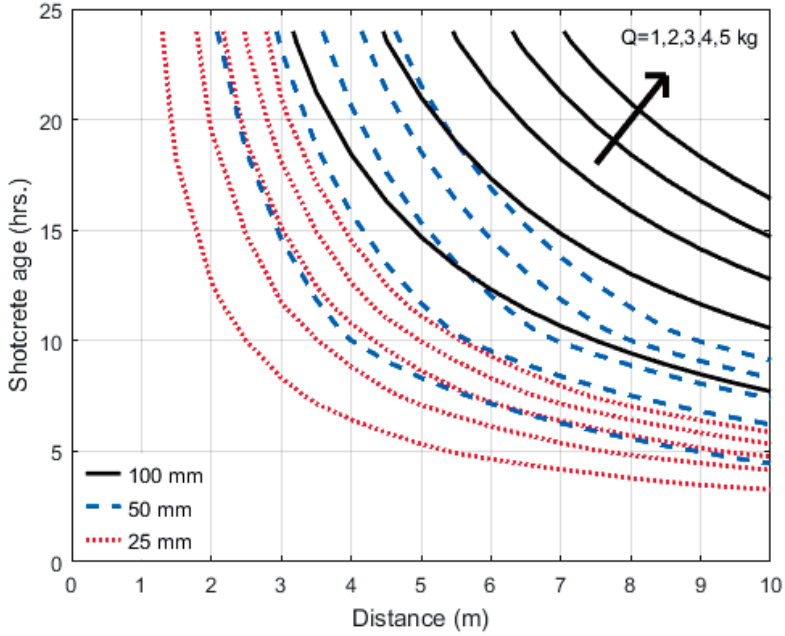


**Figure B.5:** Shotcrete type 2, Bond type 2, Rock type 1 ( $H = 0,50\text{ m}$ ,  $v_1 = 700\text{ mm/s}$ ,  $f = 1750\text{ Hz}$ ).

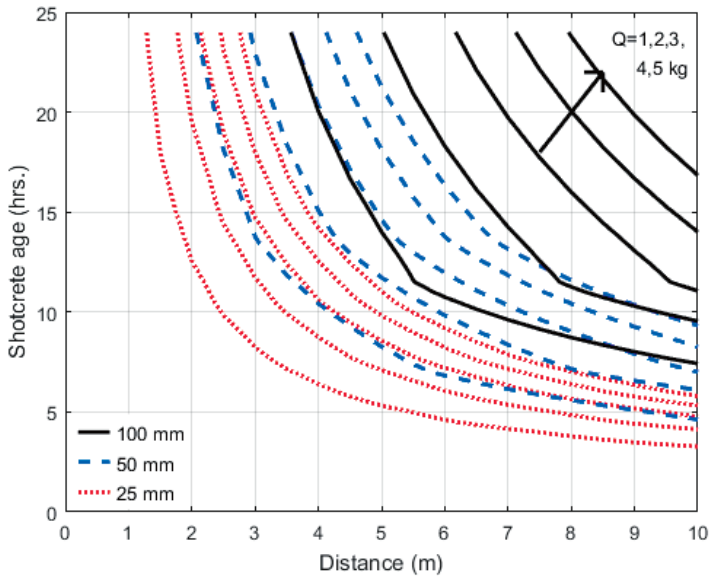


**Figure B.6:** Shotcrete type 3, Bond type 2, Rock type 1 ( $H = 0,50\text{ m}$ ,  $v_1 = 700\text{ mm/s}$ ,  $f = 1750\text{ Hz}$ ).

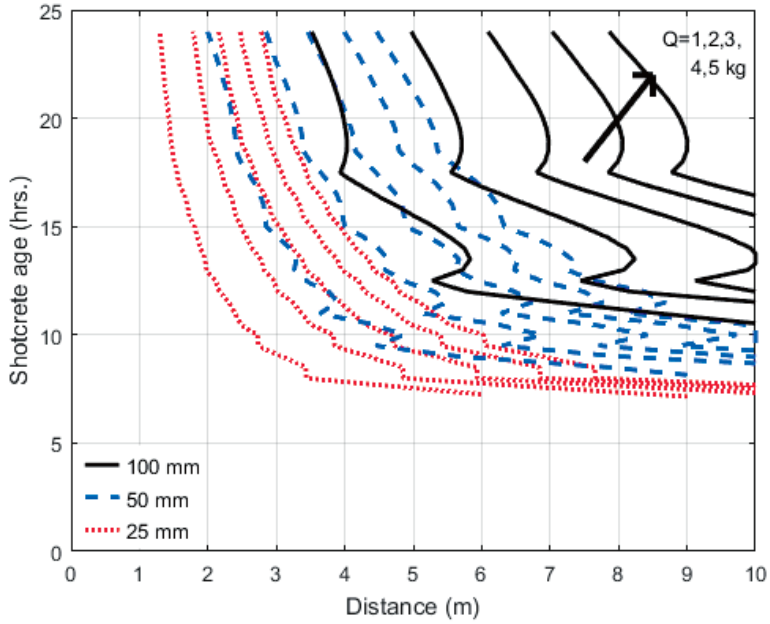
*Rock type 2*



**Figure B.7:** Shotcrete type 1, Bond type 1, Rock type 1 ( $H = 0,50$  m,  $v_1 = 1000$  mm/s,  $f = 1750$  Hz).



**Figure B.8:** Shotcrete type 2, Bond type 1, Rock type 1 ( $H = 0,50$  m,  $v_1 = 1000$  mm/s,  $f = 1750$  Hz)

*Rock type 2*

**Figure B.9:** Shotcrete type 3, Bond type 1, Rock type 1 ( $H = 0,50$  m,  $v_1 = 1000$  mm/s,  $f = 1750$  Hz).

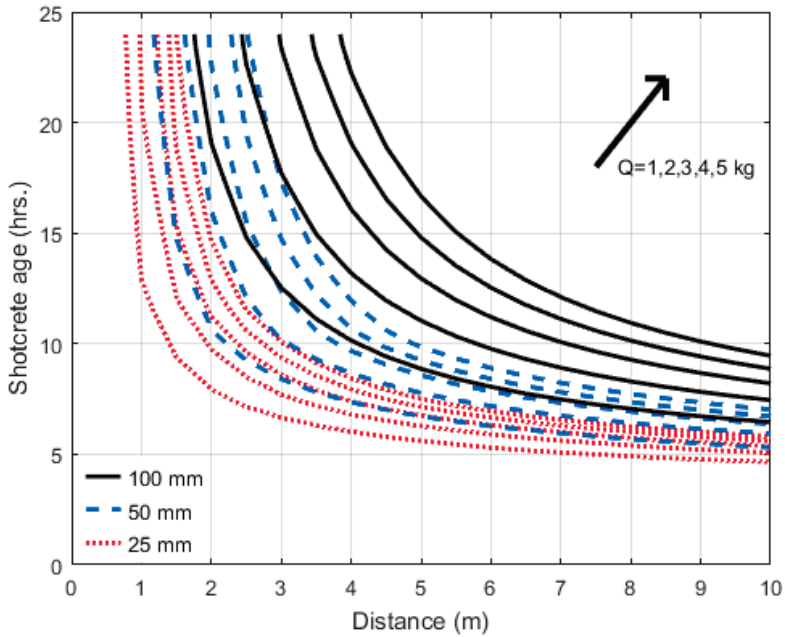


**Figure B.10:** Shotcrete type 1, Bond type 2, Rock type 1 ( $H = 0,50$  m,  $v_1 = 1000$  mm/s,  $f = 1750$  Hz).

*Rock type 2*

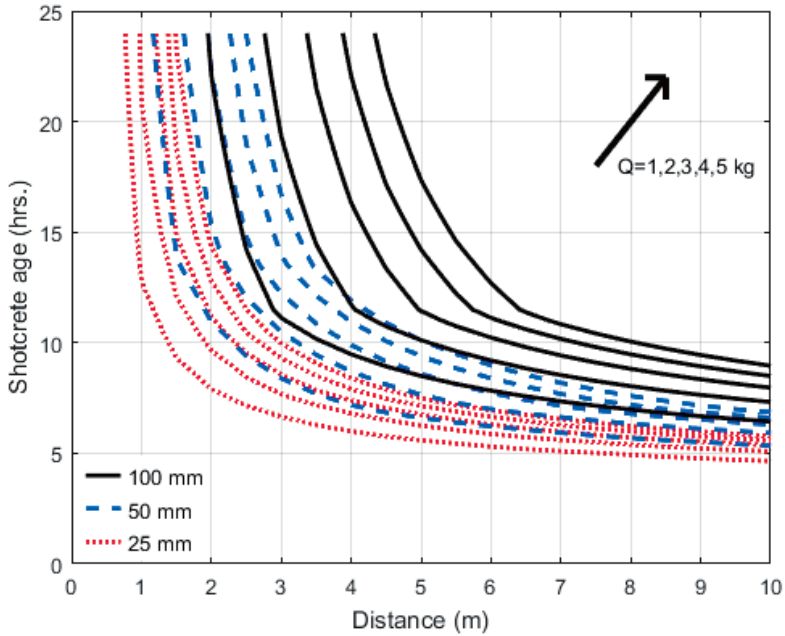


**Figure B.11:** Shotcrete type 2, Bond type 2, Rock type 1 ( $H = 0,50$  m,  $v_i = 1000$  mm/s,  $f = 1750$  Hz).

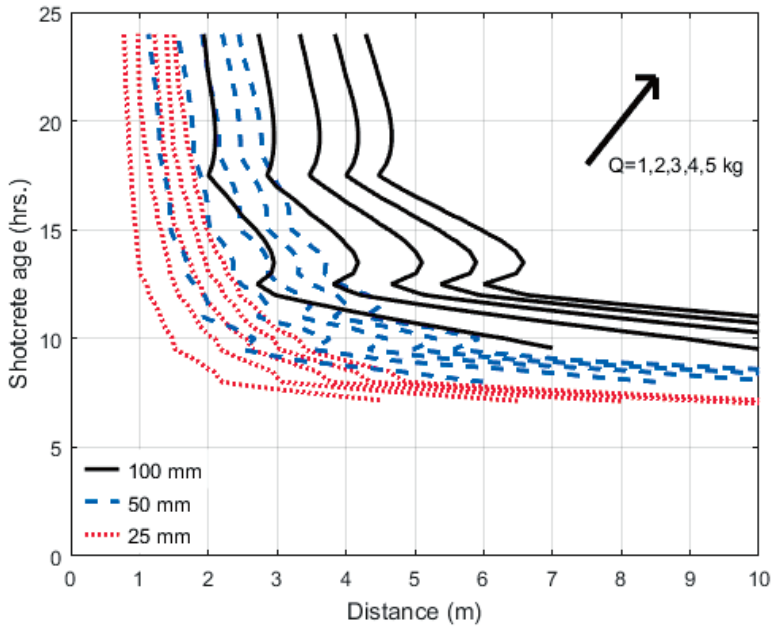


**Figure B.12:** Shotcrete type 3, Bond type 2, Rock type 1 ( $H = 0,50$  m,  $v_i = 1000$  mm/s,  $f = 1750$  Hz).

*Rock type 3 (and 5)*

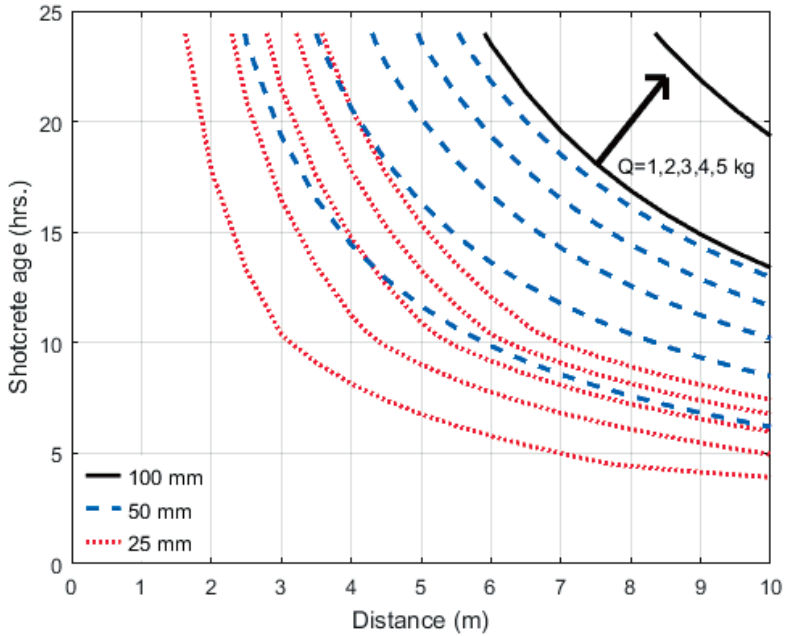


**Figure B.13:** Shotcrete type 1, Bond type 1, Rock type 3 ( $H = 0,25$  m,  $v_i = 700$  mm/s,  $f = 3500$  Hz).

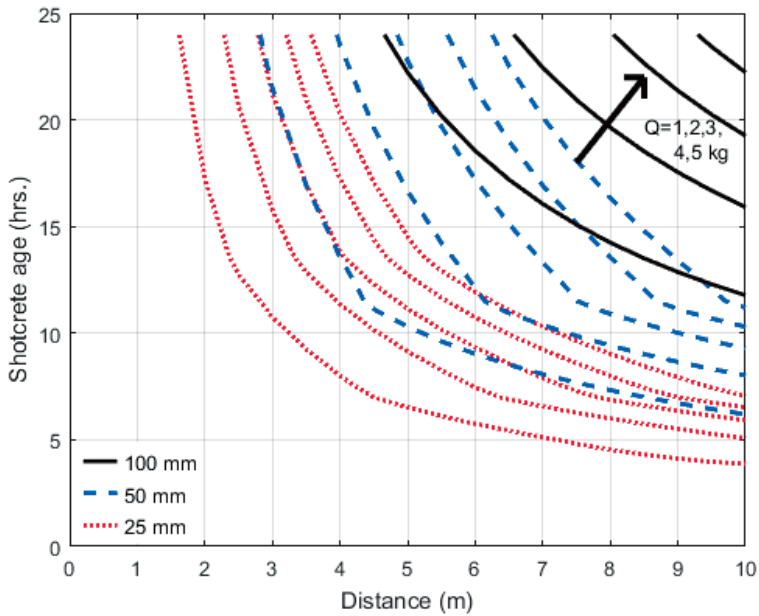


**Figure B.14:** Shotcrete type 2, Bond type 1, Rock type 3 ( $H = 0,25$  m,  $v_i = 700$  mm/s,  $f = 3500$  Hz).

*Rock type 3 (and 5)*

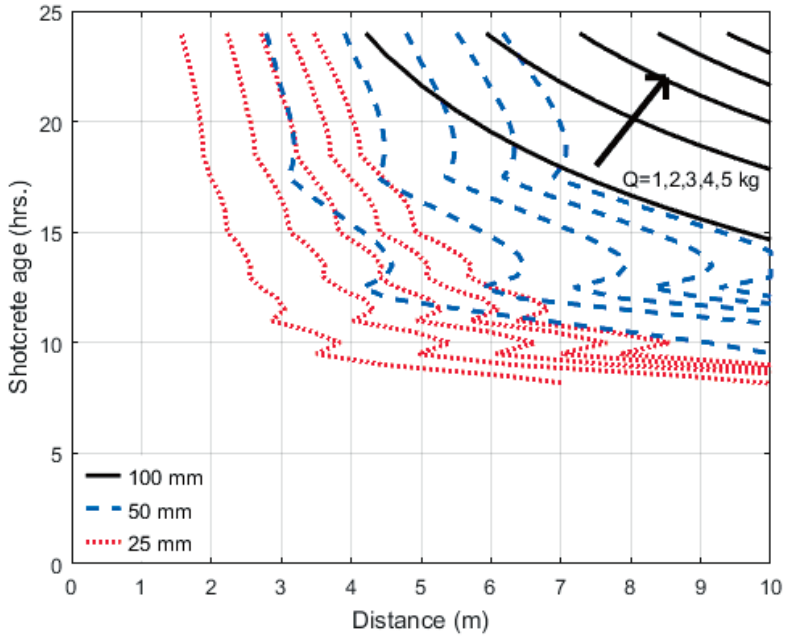


**Figure B.15:** Shotcrete type 3, Bond type 1, Rock type 3 ( $H = 0,25\text{ m}$ ,  $v_i = 700\text{ mm/s}$ ,  $f = 3500\text{ Hz}$ ).

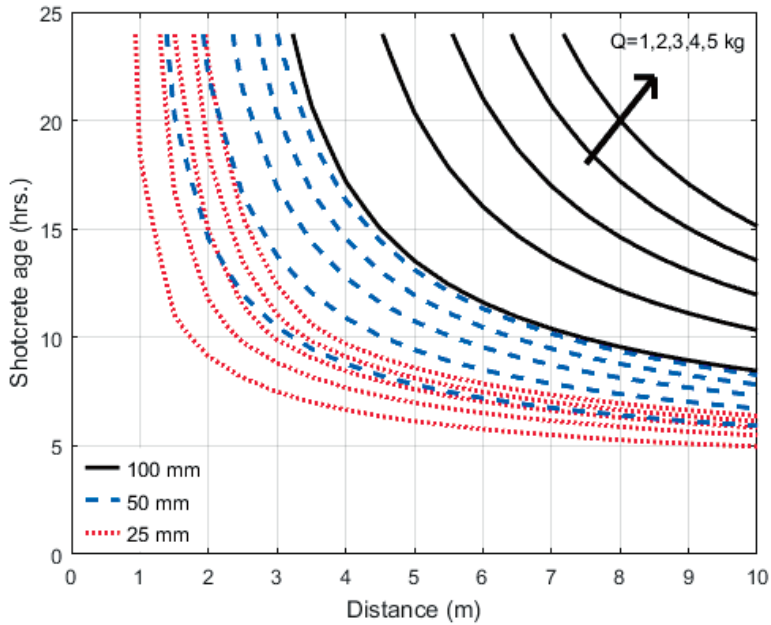


**Figure B.16:** Shotcrete type 1, Bond type 2, Rock type 3 ( $H = 0,25\text{ m}$ ,  $v_i = 700\text{ mm/s}$ ,  $f = 3500\text{ Hz}$ ).

*Rock type 3 (and 5)*

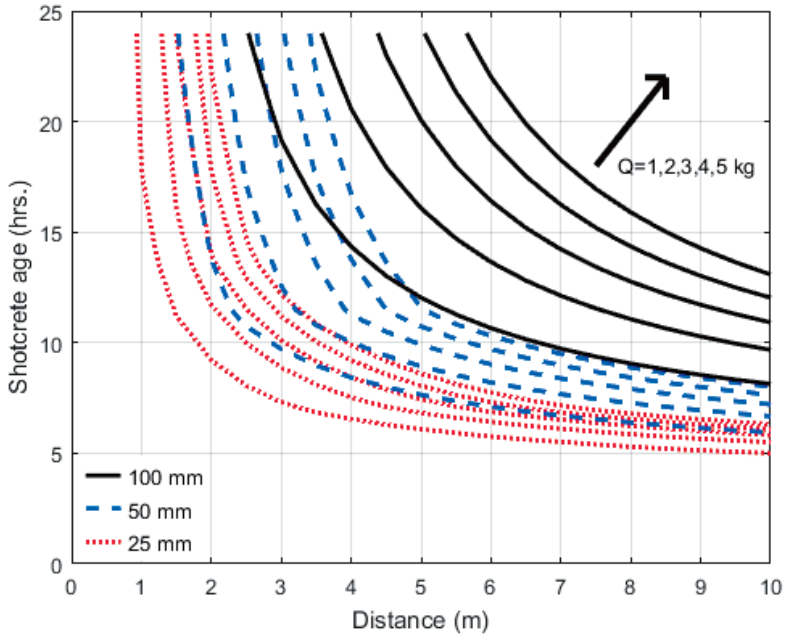


**Figure B.17:** Shotcrete type 2, Bond type 2, Rock type 3 ( $H = 0,25$  m,  $v_i = 700$  mm/s,  $f = 3500$  Hz).

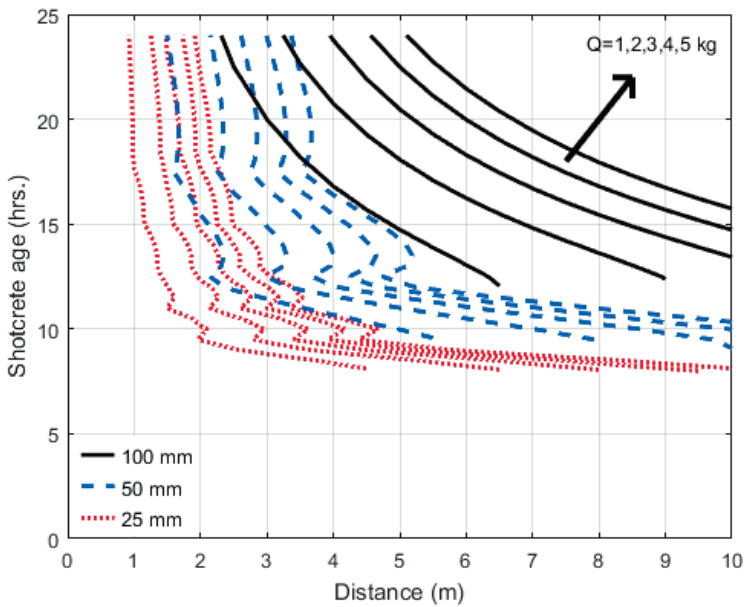


**Figure B.18:** Shotcrete type 3, Bond type 2, Rock type 3 ( $H = 0,25$  m,  $v_i = 700$  mm/s,  $f = 3500$  Hz).

*Rock type 4 (and 6)*

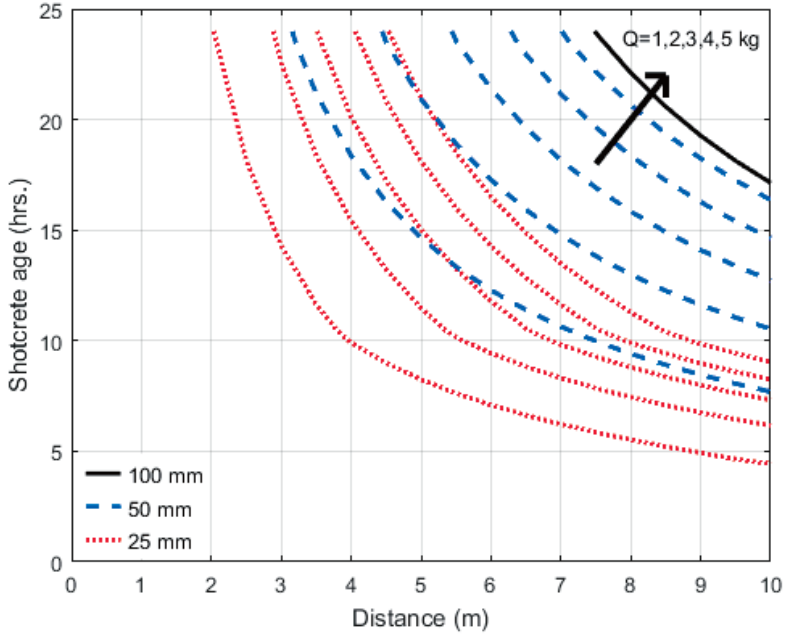


**Figure B.19:** Shotcrete type 1, Bond type 1, Rock type 3 ( $H = 0,25\text{ m}$ ,  $v_i = 1000\text{ mm/s}$ ,  $f = 3500\text{ Hz}$ ).

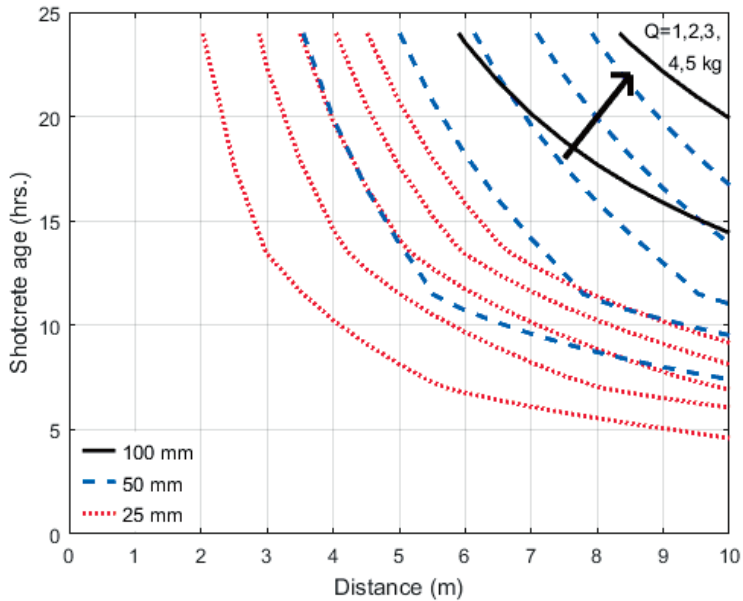


**Figure B.20:** Shotcrete type 2, Bond type 1, Rock type 3 ( $H = 0,25\text{ m}$ ,  $v_i = 1000\text{ mm/s}$ ,  $f = 3500\text{ Hz}$ ).



*Rock type 4 (and 6)*

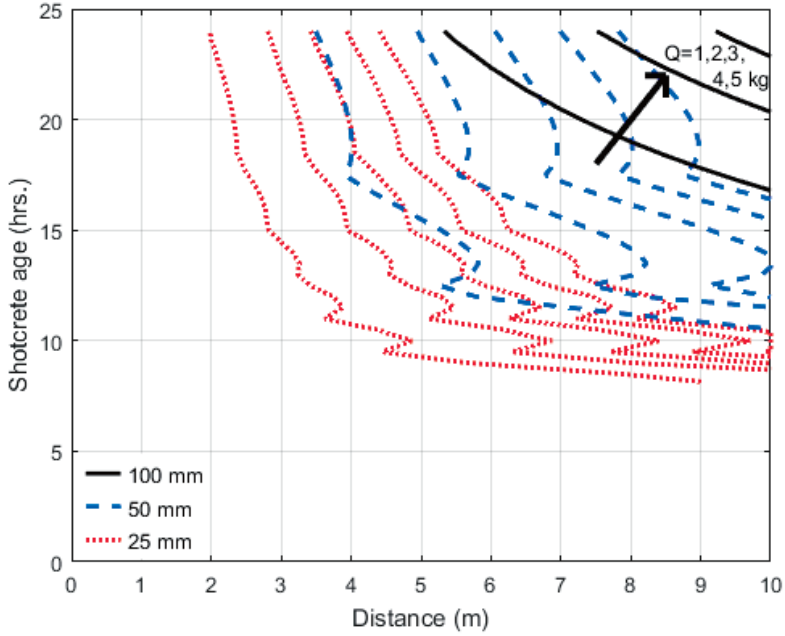


**Figure B.21:** Shotcrete type 3, Bond type 1, Rock type 3 ( $H = 0,25$  m,  $v_i = 1000$  mm/s,  $f = 3500$  Hz).

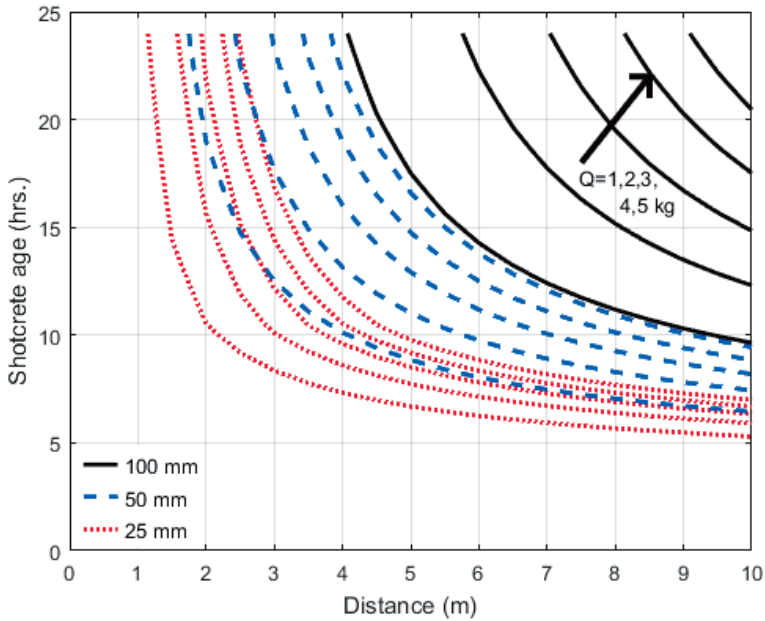


**Figure B.22:** Shotcrete type 1, Bond type 2, Rock type 3 ( $H = 0,25$  m,  $v_i = 1000$  mm/s,  $f = 3500$  Hz).

*Rock type 4 (and 6)*

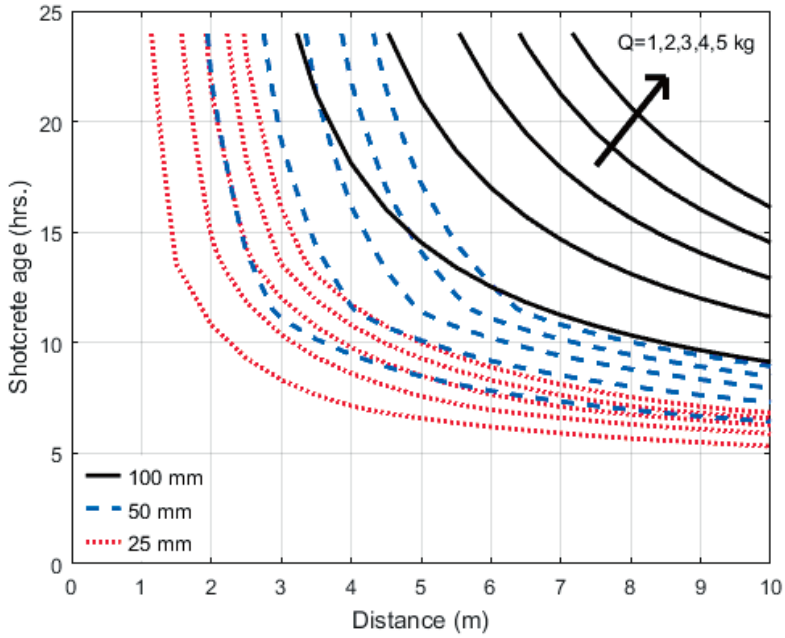


**Figure B.23:** Shotcrete type 2, Bond type 2, Rock type 3 ( $H = 0,25$  m,  $v_i = 1000$  mm/s,  $f = 3500$  Hz).

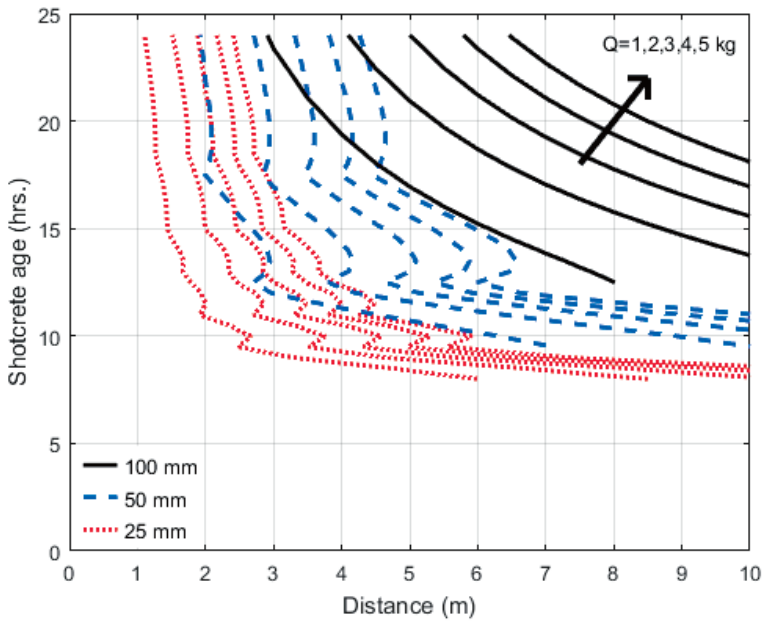


**Figure B.24:** Shotcrete type 3, Bond type 2, Rock type 3 ( $H = 0,25$  m,  $v_i = 1000$  mm/s,  $f = 3500$  Hz).

## Rock type 7

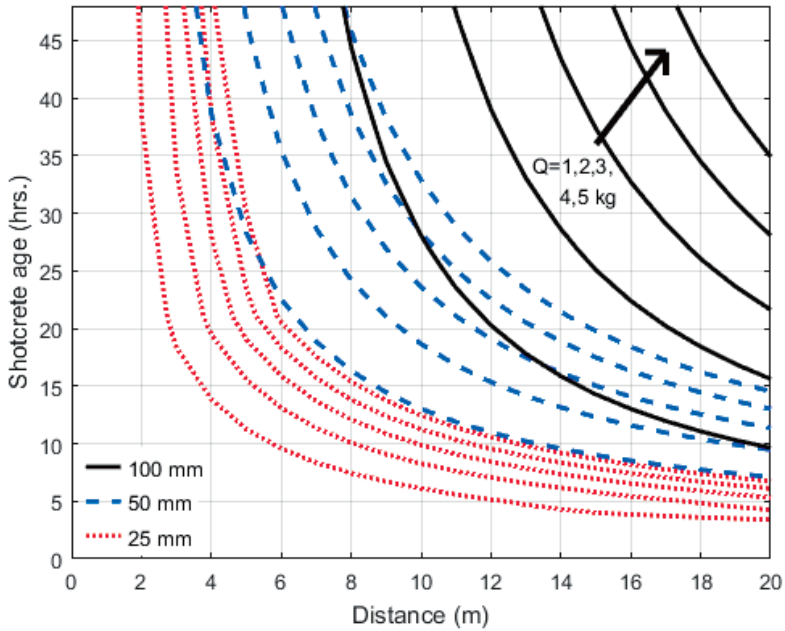


Figure B.25: Shotcrete type 1, Bond type 1, Rock type 7 ( $H = 0,25$  m,  $v_i = 700$  mm/s,  $f = 7000$  Hz).

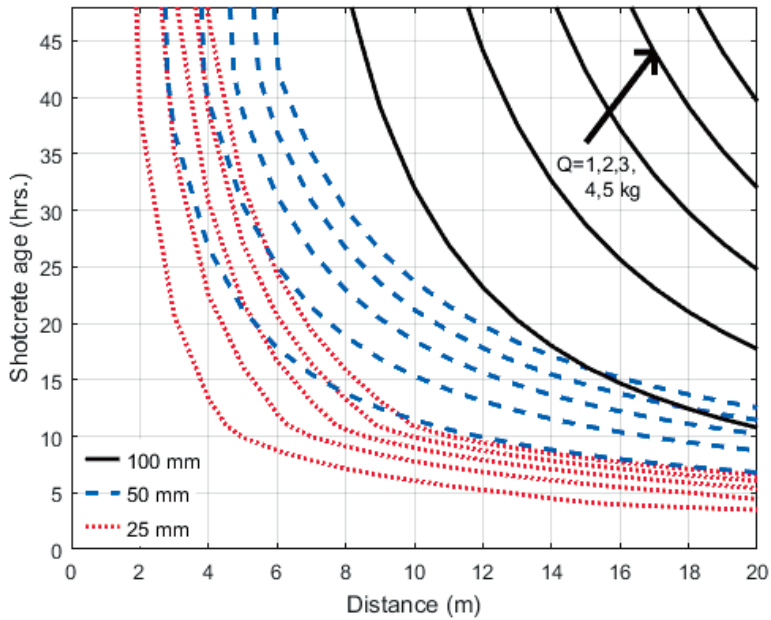
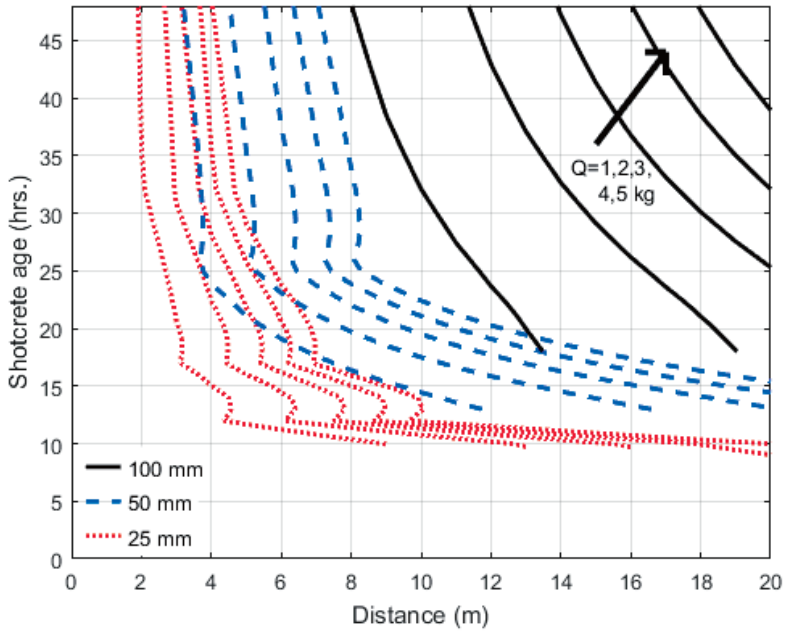
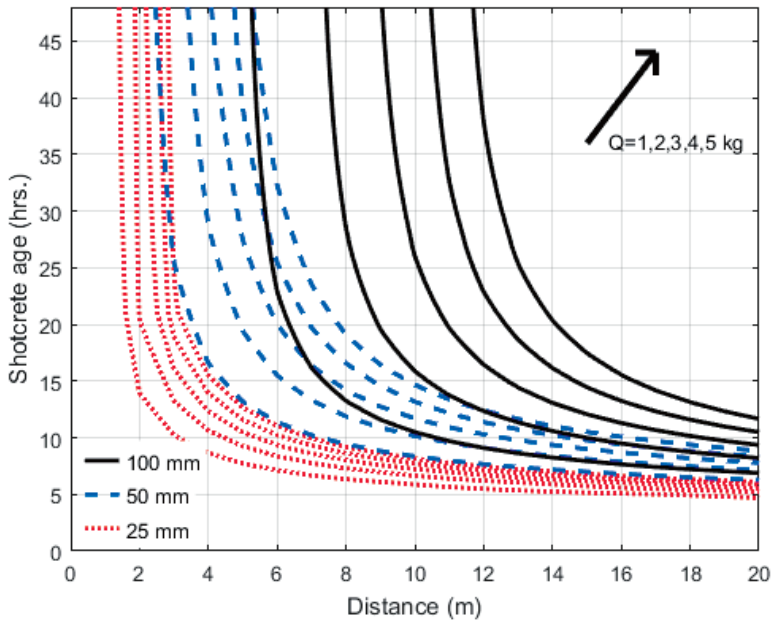


Figure B.26: Shotcrete type 2, Bond type 1, Rock type 7 ( $H = 0,25$  m,  $v_i = 700$  mm/s,  $f = 7000$  Hz).

## Rock type 7



**Figure B.27:** Shotcrete type 3, Bond type 1, Rock type 7 ( $H = 0,25$  m,  $v_i = 700$  mm/s,  $f = 7000$  Hz).



**Figure B.28:** Shotcrete type 1, Bond type 2, Rock type 7 ( $H = 0,25$  m,  $v_i = 700$  mm/s,  $f = 7000$  Hz).

## Rock type 7

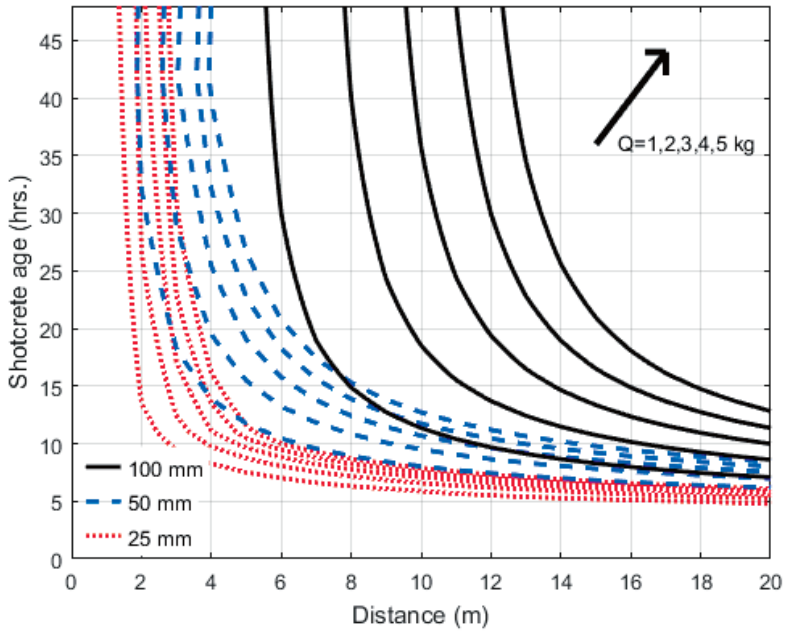


Figure B.29: Shotcrete type 2, Bond type 2, Rock type 7 ( $H = 0,25$  m,  $v_i = 700$  mm/s,  $f = 7000$  Hz).

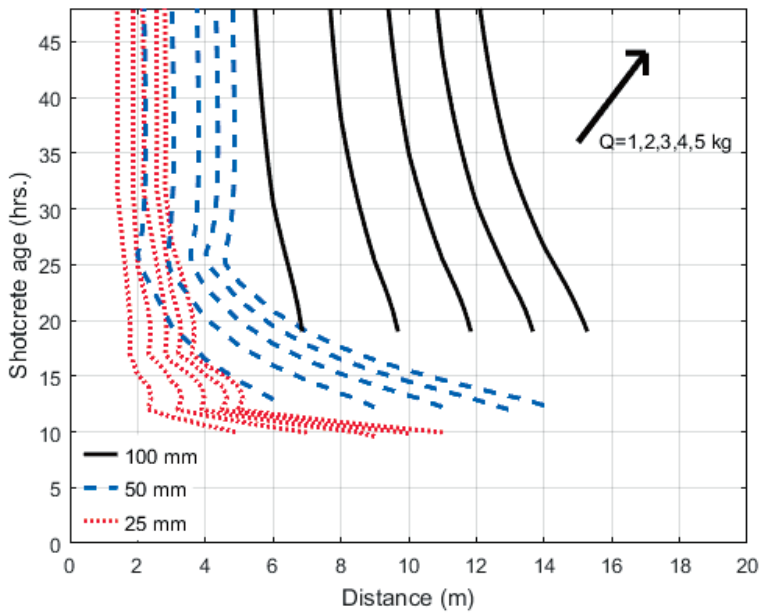
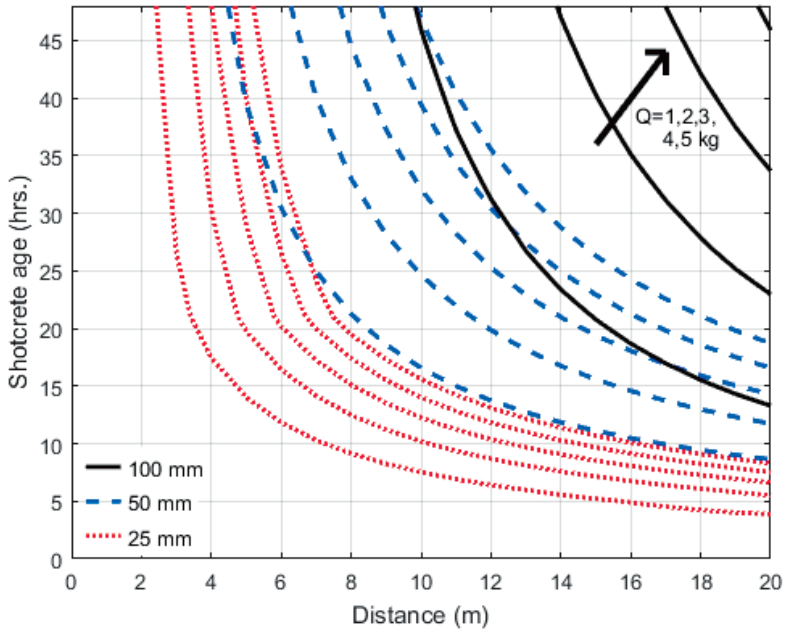
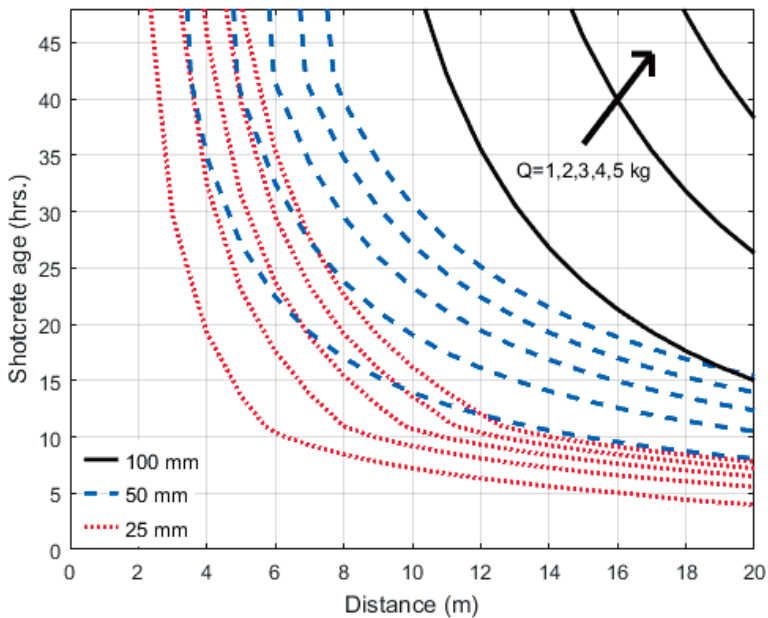


Figure B.30: Shotcrete type 3, Bond type 2, Rock type 7 ( $H = 0,25$  m,  $v_i = 700$  mm/s,  $f = 7000$  Hz).

## Rock type 8



**Figure B.31:** Shotcrete type 1, Bond type 1, Rock type 8 ( $H = 0,25$  m,  $v_i = 1000$  mm/s,  $f = 7000$  Hz).



**Figure B.32:** Shotcrete type 2, Bond type 1, Rock type 8 ( $H = 0,25$  m,  $v_i = 1000$  mm/s,  $f = 7000$  Hz).

## Rock type 8

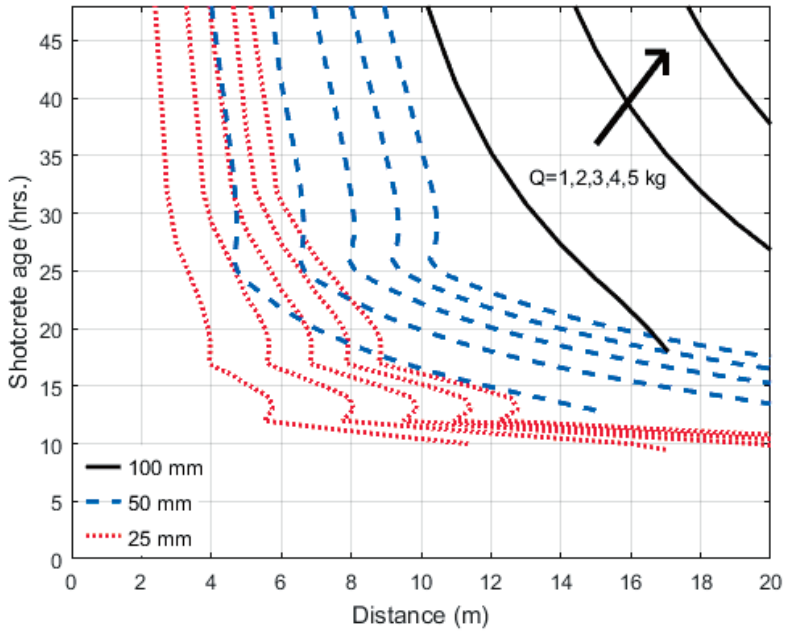


**Figure B.33:** Shotcrete type 3, Bond type 1, Rock type 8 ( $H = 0,25$  m,  $v_i = 1000$  mm/s,  $f = 7000$  Hz).

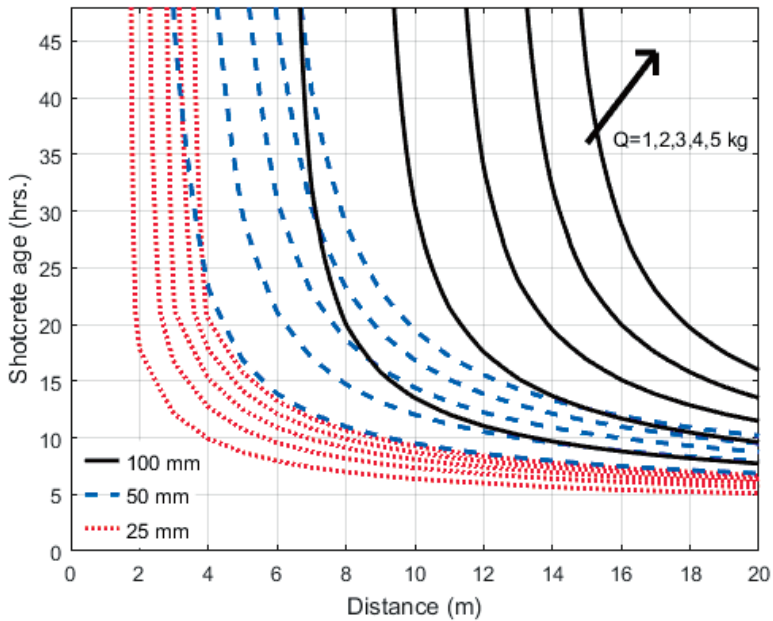


**Figure B.34:** Shotcrete type 1, Bond type 2, Rock type 8 ( $H = 0,25$  m,  $v_i = 1000$  mm/s,  $f = 7000$  Hz).

## Rock type 8

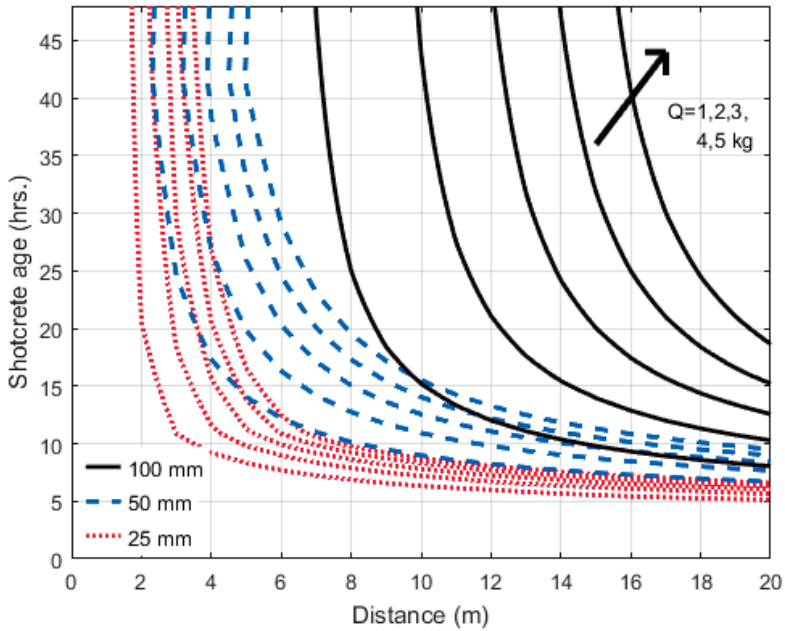


Figure B.35: Shotcrete type 2, Bond type 2, Rock type 8 ( $H = 0,25\text{ m}$ ,  $v_i = 1000\text{ mm/s}$ ,  $f = 7000\text{ Hz}$ ).

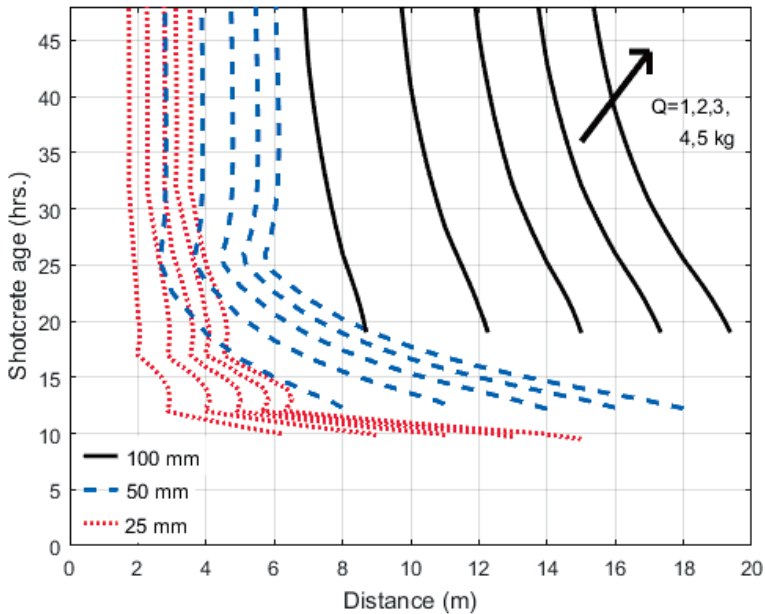
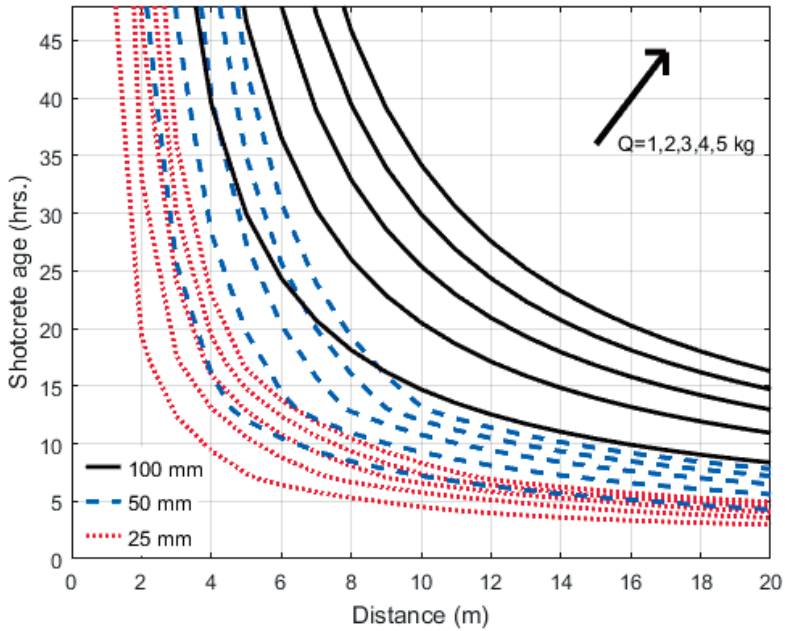


Figure B.36: Shotcrete type 3, Bond type 2, Rock type 8 ( $H = 0,25\text{ m}$ ,  $v_i = 1000\text{ mm/s}$ ,  $f = 7000\text{ Hz}$ ).



## Rock type 9



**Figure B.37:** Shotcrete type 1, Bond type 1, Rock type 9 ( $H = 0,50$  m,  $v_l = 830$  mm/s,  $f = 3150$  Hz).

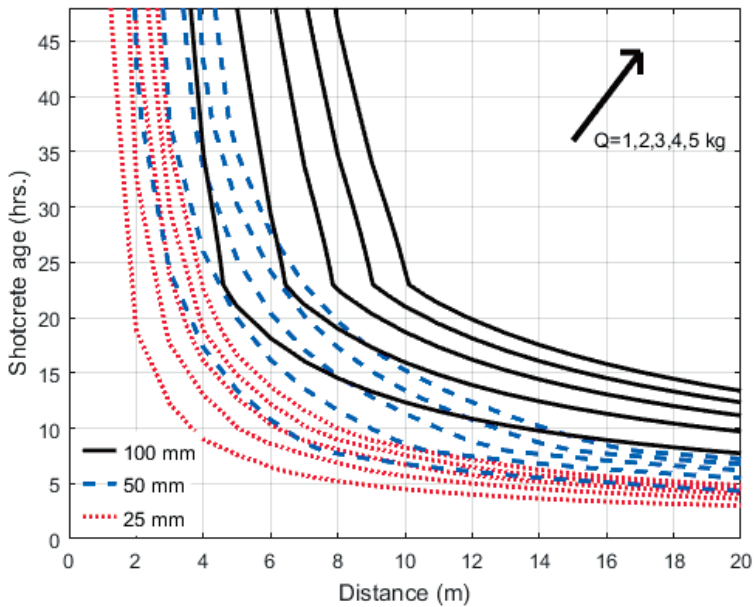


**Figure B.38:** Shotcrete type 2, Bond type 1, Rock type 9 ( $H = 0,50$  m,  $v_l = 830$  mm/s,  $f = 3150$  Hz).

## Rock type 9

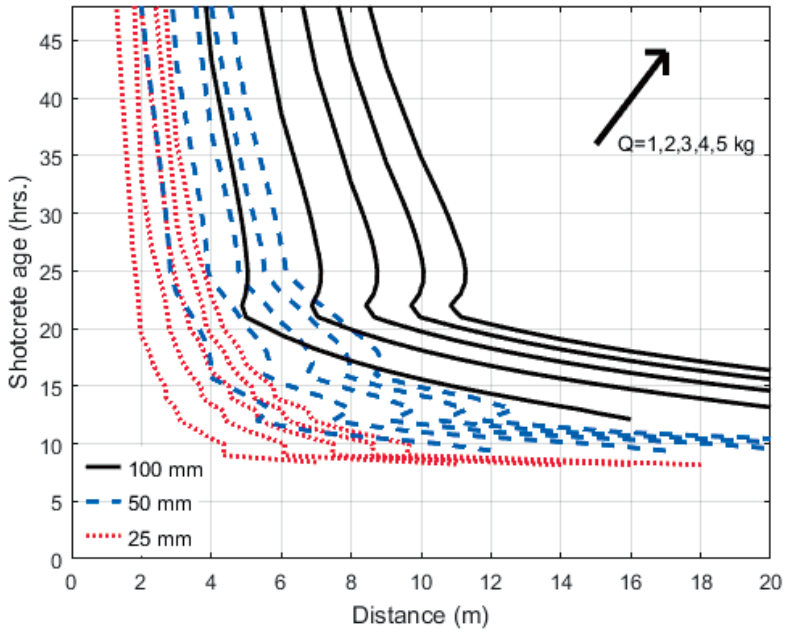


**Figure B.39:** Shotcrete type 3, Bond type 1, Rock type 9 ( $H = 0,50$  m,  $v_i = 830$  mm/s,  $f = 3150$  Hz).

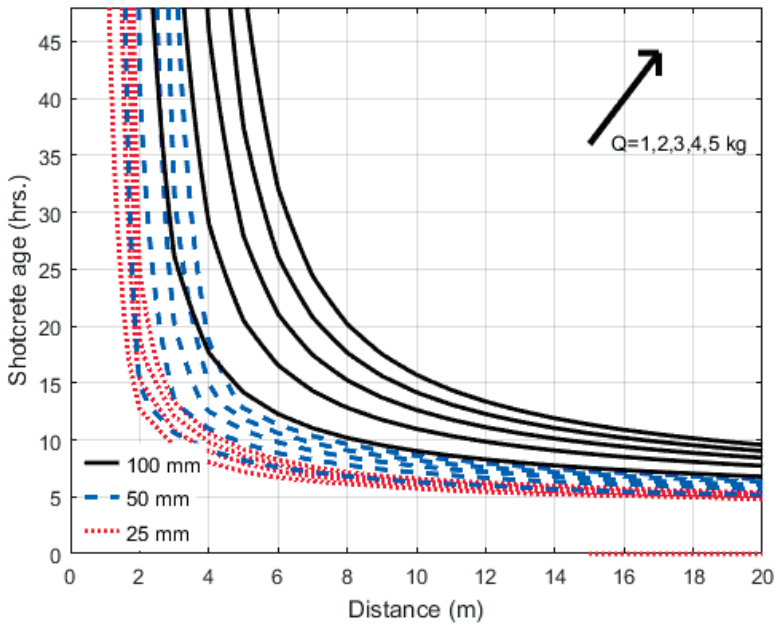


**Figure B.40:** Shotcrete type 1, Bond type 2, Rock type 9 ( $H = 0,50$  m,  $v_i = 830$  mm/s,  $f = 3150$  Hz).

## Rock type 9

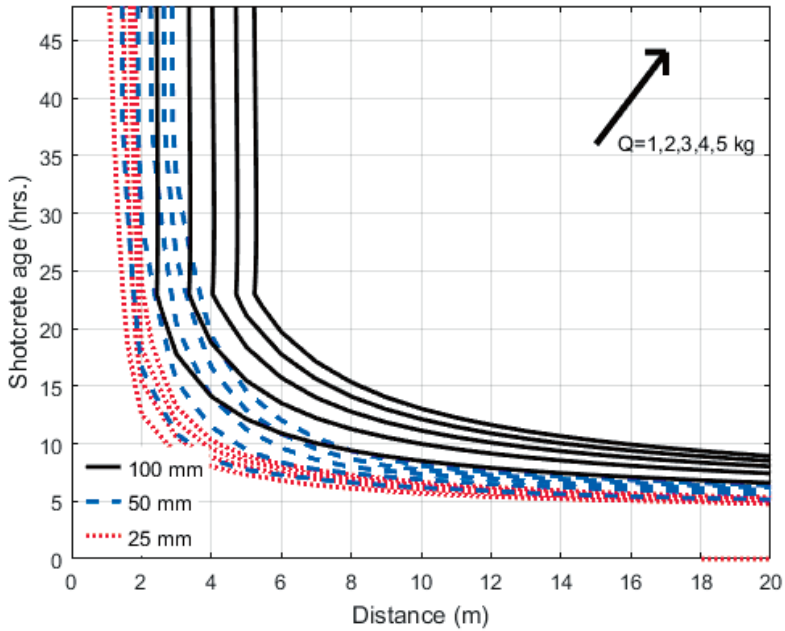


**Figure B.41:** Shotcrete type 2, Bond type 2, Rock type 9 ( $H = 0,50$  m,  $v_i = 830$  mm/s,  $f = 3150$  Hz).

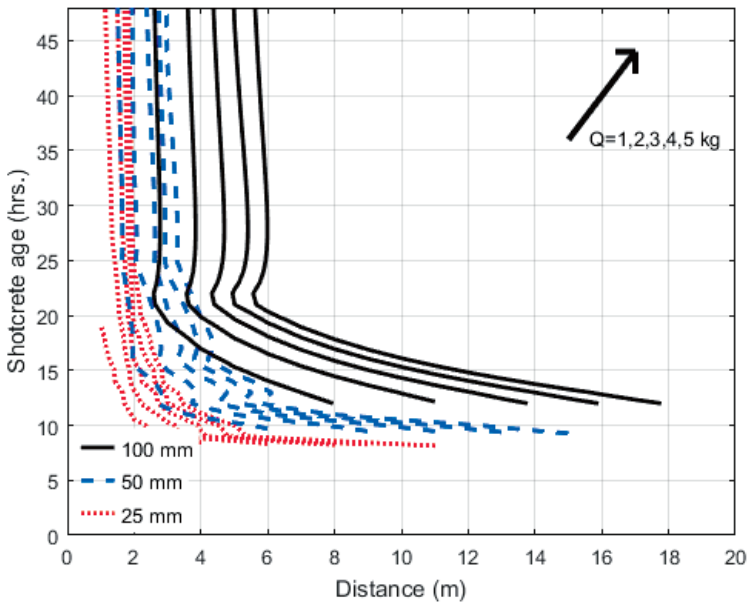


**Figure B.42:** Shotcrete type 3, Bond type 2, Rock type 9 ( $H = 0,50$  m,  $v_i = 830$  mm/s,  $f = 3150$  Hz).

## Rock type 10

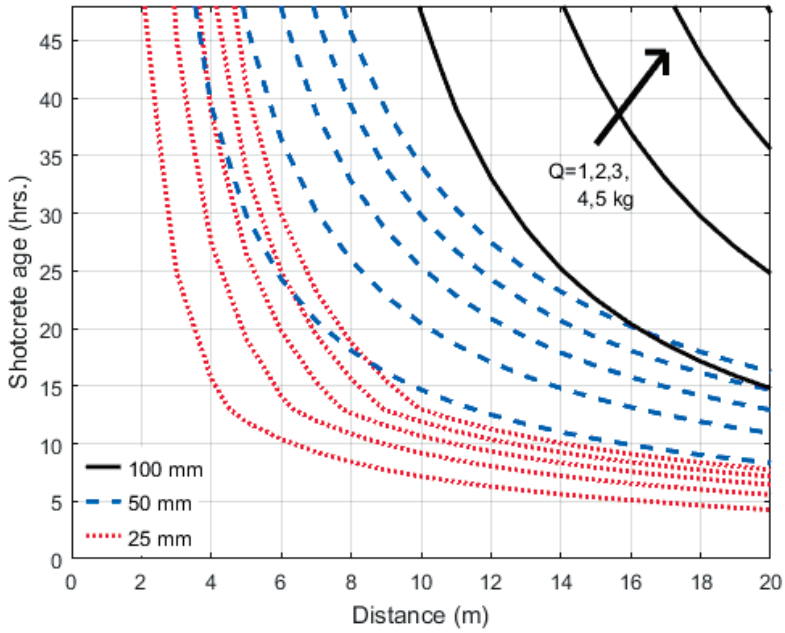


**Figure B.43:** Shotcrete type 1, Bond type 1, Rock type 10 ( $H = 0,25$  m,  $v_1 = 830$  mm/s,  $f = 6300$  Hz).

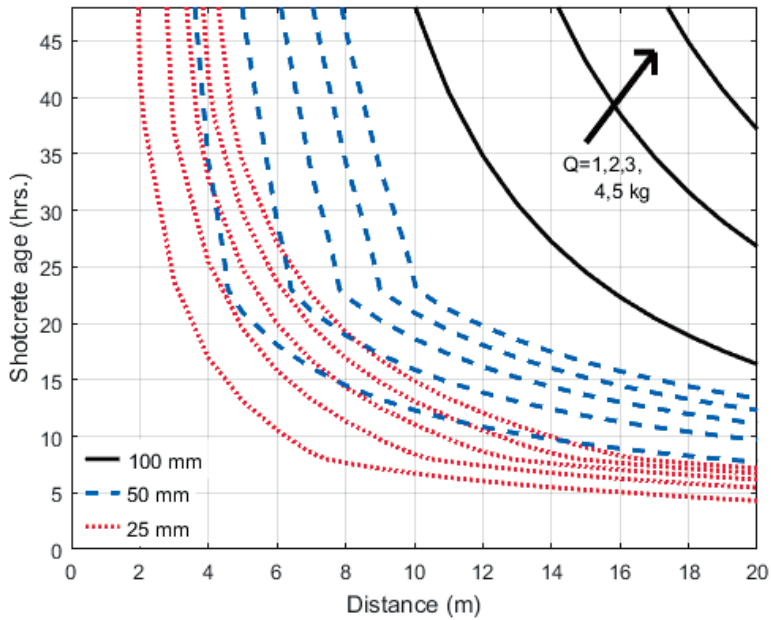


**Figure B.44:** Shotcrete type 2, Bond type 1, Rock type 10 ( $H = 0,25$  m,  $v_1 = 830$  mm/s,  $f = 6300$  Hz).

## Rock type 10

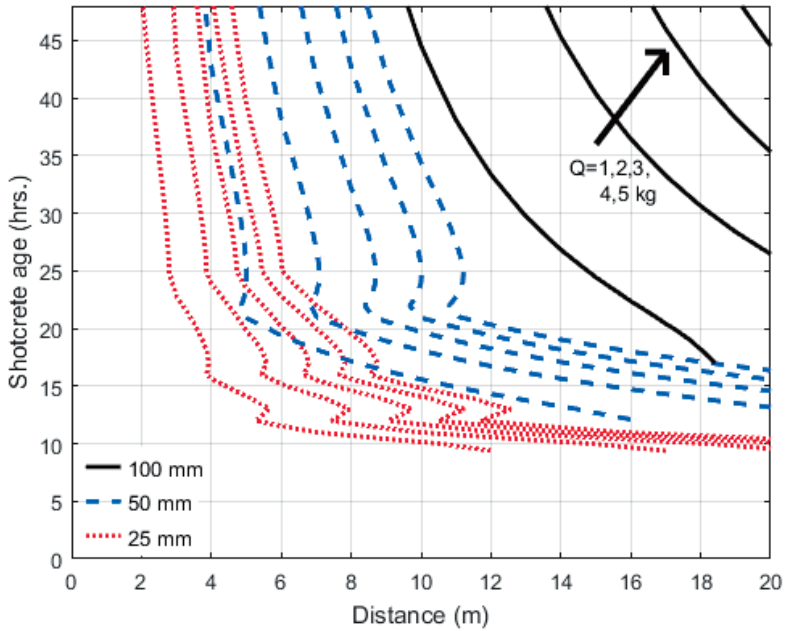


Figure B.45: Shotcrete type 3, Bond type 1, Rock type 10 ( $H = 0,25$  m,  $v_1 = 830$  mm/s,  $f = 6300$  Hz).

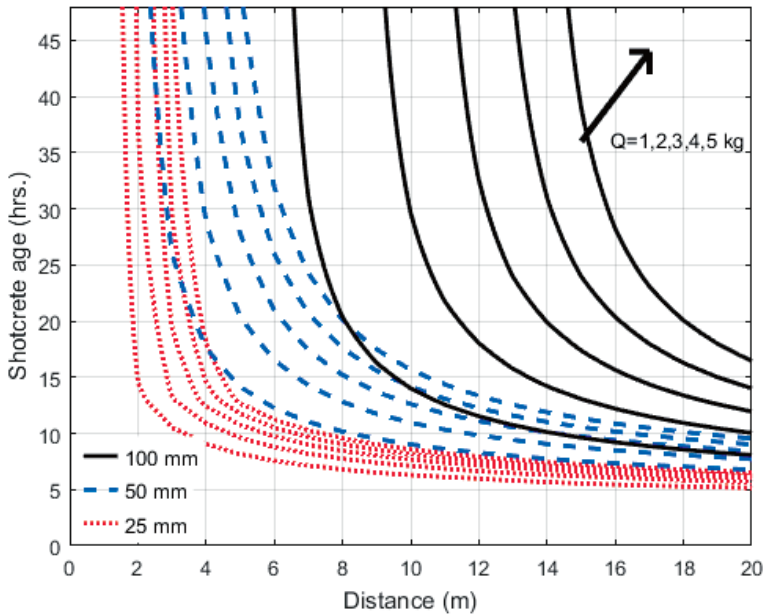
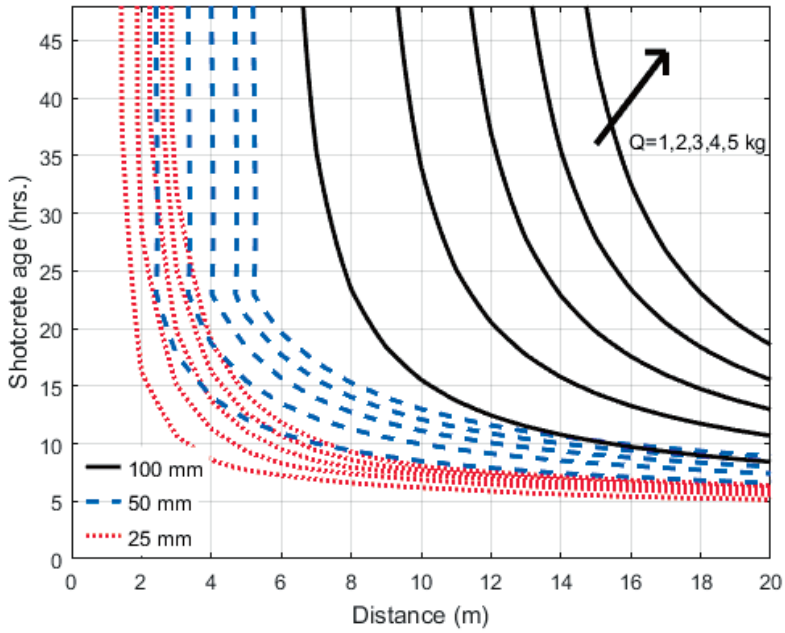
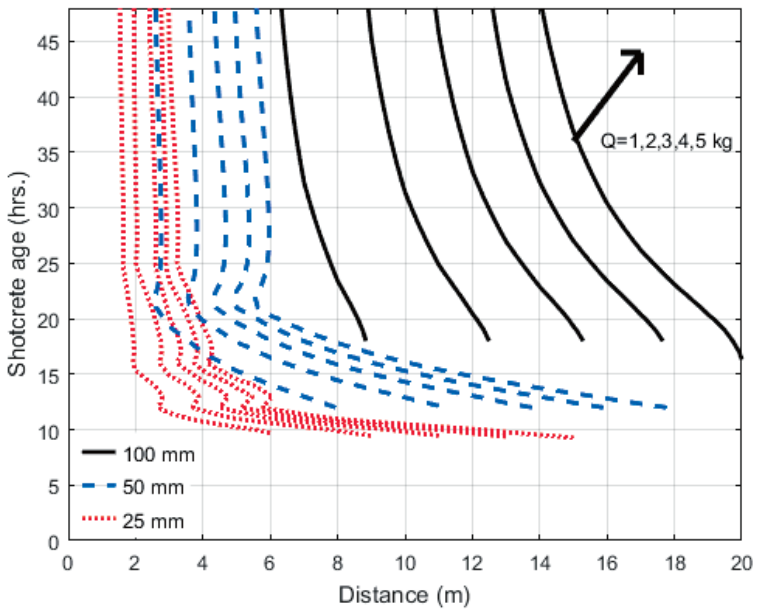


Figure B.46: Shotcrete type 1, Bond type 2, Rock type 10 ( $H = 0,25$  m,  $v_1 = 830$  mm/s,  $f = 6300$  Hz).

## Rock type 10



**Figure B.47:** Shotcrete type 2, Bond type 2, Rock type 10 ( $H = 0,25$  m,  $v_l = 830$  mm/s,  $f = 6300$  Hz).



**Figure B.48:** Shotcrete type 3, Bond type 2, Rock type 10 ( $H = 0,25$  m,  $v_l = 830$  mm/s,  $f = 6300$  Hz).



Box 55545  
SE-102 04 Stockholm

info@befoonline.org • www.befoonline.org  
Visiting address: Sturegatan 11, Stockholm

ISSN 1104-1773